Meroplanktic phytoplankton play a crucial role in responding to peak discharge events in the middle lowland section of the Loire River (France)

Alexandrine Pannard, Camille Minaudo, Maria Leitao, Andras Abonyi, Florentina Moatar, Nathalie Gassama

Meroplanktic phytoplankton play a crucial role in responding to peak discharge events in the middle lowland section of the Loire River (France)

Meroplanktic phytoplankton play a crucial role in responding to peak discharge events in the middle lowland section of the Loire River (France)

Alexandrine Pannard[1], Camille Minaudo[2], Maria Leitao[3], Andras Abonyi[4,5,6], Florentina Moatar[7] and Nathalie Gassama[8]

1. University of Rennes, UMR 6553 ECOBIO, Rennes, France
2. Department of Evolutionary Biology, Ecology and Environmental Sciences, University of Barcelona, Av. Diagonal 643, Barcelona 08028, Spain
3. Bi-Eau, 15 rue Lainé-Laroche, Angers, France
4. Institute of Aquatic Ecology, Centre for Ecological Research, Karolina street 29, Budapest, Hungary
5. MTA-ÖK "Lendület" Momentum Fluvial Ecology Research Group, Karolina street 29, Budapest, Hungary
6. WasserCluster Lunz, Dr. Kupelwieser-Prom. 5, Lunz am See, Austria
7. INRAE, UR RiverLy - Centre de Lyon-Grenoble Auvergne-Rhône-Alpes, Villeurbanne, France
8. University of Tours, E.A. 6293 GéHCO, Tours, France.

Corresponding author: alexandrine.pannard@univ-rennes.fr

Abstract

Meteorological and hydrological forcings influence phytoplankton at very short time scales. The effect of turbulence, dilution, light and nutrients are highly dynamic. Yet, our knowledge of short-term phytoplankton dynamics associated with discharge disturbances and nutrient inputs remains elusive, especially in large rivers.

Based on every three-day monitoring, we studied phytoplankton in the middle Loire River (France) and related to the daily variations in water discharge and the physical and chemical parameters. We focused on summer phytoplankton (2013 and 2014), where dissolved inorganic phosphorus concentration was potentially limiting growth. We identified eight discharge events, which increased suspended matter concentration and decreased chlorophyll-a concentration. The most significant

environmental drivers of phytoplankton composition were discharge and water temperature, a sensitive proxy for meteorological forcing at short-time scale.

The phytoplankton composition responded to changes in hydrology along with three distinct assemblage types, where even small water discharge increase induced a community response. Meroplanktic algae being able to withstand sedimentation and resuspension could take advantage of hydrological peaks, following the benthic retention hypothesis. Our results suggest that short-term dynamics are crucial to understanding community organisation and functioning in large river plankton, with meroplankton playing a decisive role in maintaining phytoplankton diversity and ecosystem functioning.

Keywords: large rivers; short-term events; benthic retention hypothesis; Reynolds' phytoplankton functional groups; functional traits

Introduction

Large rivers are critical players in the biogeochemical dynamics, exerting control over the transport of organic matter and associated chemical elements along the land-sea continuum. Large spatial and temporal variations occur in hydrology and biogeochemical processes in rivers, which also influence the diversity of aquatic communities (Johnson et al., 1995). Large rivers exceeds the sixth river order (Wehr & Descy, 1998) with extended braided arms towards the lowland river section. Their hydrology is subjected to significant variations in discharge in response to meteorological variations and water flow management. Water discharge also controls connectivity among adjacent pools composed by water bodies with different water quality. The longitudinal component from the headwaters to the lowland reach can be described by a continuous change in environmental conditions, well summarised in the 'River Continuum Concept - RCC' (Vannote et al., 1980). The RCC also provides a natural gradient to scale the diversity of aquatic communities. The RCC describes changes in river metabolism, in the type of primary producers and the macro-invertebrates and fishes' community structure, associated with changes in the slope (current velocity), allochthonous inputs, light exposure and water residence time. The large lowland river sections are influenced by upstream processes and aquatic communities, with

2

phytoplankton dominance mainly from the middle river section (Reynolds & Descy, 1996). Temporal fluctuations associated with river discharge should affect the taxonomic and functional diversity of aquatic communities, by connecting benthic and planktic communities, in accordance with the benthic retention hypothesis (Istvànovics & Honti, 2011). This latter suggests that fast-sinking meroplanktic diatoms can take advantage of sedimentation and resuspension if the retention time is sufficiently short and can compensate against light deficient conditions (Istvànovics & Honti, 2011). How this hypothesis applies to other taxonomic groups, such as coccal green algae that may be favoured during summer low flow conditions, remains unclear.

Phytoplankton play a crucial role in the ecology and functioning of large rivers, reproducing within river (Wu et al., 2011) and exhibiting a rapid response time to environmental conditions ranging from a few hours to a few days. Phytoplankton biomass and composition are controlled by a set of biotic and abiotic factors, such as flushing rate (Reynolds et al., 1994), turbulence (Bormans et al., 2004), light availability into the water column (linked to atmospheric conditions, turbidity and river depth) (Várbíró et al., 2018), water temperature (Peterson & Stevenson, 1989), nutrient availability (Minaudo et al., 2021), competition for nutrients with macrophytes (Sabater et al., 2008), and grazing by zooplankton (Lair & Reyes-Marchant, 1997). Studies often identify and rank controlling factors at a seasonal time scale, focusing on hydrological forcing with high *versus* low-flow periods, on bottom-up aspects (seasonal changes in resource availability) or, more exceptionally on top-down control (Picard & Lair, 2005). While the seasonal and longitudinal dynamics of phytoplankton have been well studied in large rivers (Reynolds & Descy, 1996; Istvánovics et al., 2010), short-term dynamics associated with discharge forcing, have mainly been neglected. Biological responses, in terms of growth and biomass, are known (Kiss et al., 1996), and are increasingly studied based on high-frequency data (Bowes et al., 2016; Pathak et al., 2021). However, much less has been derived in terms of community responses (Dubelaar et al., 2004).

Changes in phytoplankton assemblages result from two key interacting processes (Cloern, 1996; Loreau & Mouquet, 1999; Hiltunen et al., 2006): (1) the allogenic processes (also called larger-scale or regional processes), with physical transport, mixing and water advection, which mix populations of different origins and waters with different chemical compositions; (2) the autogenic processes (also called local

3

processes), with biological processes such as species-dependent growth and losses due to competition, predation or response to abiotic changes. Temporal response to allogenic processes is considered immediate whereas autogenic processes need time to produce a visible response in the ecosystem (Reynolds, 1984; Cloern, 1996; Pannard et al., 2008b).

In lakes, it is known that short-term dynamic of phytoplankton is mainly controlled by wind forcing (Carrick et al., 1993; Reynolds, 2006; Winder et al., 2008). Wind-induced mixing controls the physical and chemical environment (resource availability, stratification intensity, deepening on the mixed layer) and the development of species adapted to well-mixed conditions (Pannard et al., 2008a). In temperate lakes, the short-term dynamic nests into the seasonal dynamic, leading to a new community structure without any return to the previous one, because of constantly changing environmental conditions (thermocline depth or temperature, for instance). Such 'resetting events' are more common in tropical lakes (Lewis, 1978).

In coastal areas, the short-term dynamic of phytoplankton is also controlled by mixing events with estuarine waters due to windy circumstances, river flow and tidal dynamics (Lohrenz et al., 2003). Mixing events lead to an abrupt change in the total phytoplankton biomass and concentration of dominant species with irregularly high growth rates (Pannard et al., 2008b). Consequently, varying intensity and frequency in physical forcing help maintain high phytoplankton diversity in lakes and coastal waters by mixing populations, suppressing dominance and favouring rare species.

Water discharge can swiftly regulate autogenic and allogenic processes in river phytoplankton. An elevation in river discharge can alter environmental conditions such as turbulence and turbidity, while facilitating the connection of neighbouring water bodies with distinct nutrient loads and communities, including the benthic-pelagic interface (Istvànovics & Honti, 2011). During flood events, phytoplankton is enriched by meroplankton, which refers to benthic and epiphytic species that have been resuspended, and species from adjacent aquatic ecosystems reconnected by hydrological forcing. Rojo et al. (1994) have shown that meroplankton can represent a significant fraction of the total phytoplankton biomass (up to 50% of suspended taxa). Benthic and epiphytic taxa observed in phytoplankton should be a good proxy of river discharge peak events. Mixing-induced meroplankton occurrence should increase diversity and at the same time may help maintain rare species.

4

River discharge is a crucial driver of phytoplankton dynamics and should promote diversity maintenance by i) transporting new species from adjacent river pools and benthic areas, ii) diluting the resident community, dampening the competitive exclusion by dominant species and therefore sustaining rare species, iii) changing light by increasing turbidity, thus limiting growth except for shade-adapted species, iv) increasing nutrient availability, either directly through nutrient inputs from the catchment area, or indirectly by reducing the boundary layer around large cells through turbulence (Barton et al., 2014) and by reducing the competition for nutrients when dominant species are suppressed. While nutrient pulses favour fast-growing species, large cells might take advantage of these short-term events, thanks to nutrient storage. Thus, species-specific characteristics (i.e. traits) should primarily reflect the species- and community-level responses to discharge-mediated disturbances.

Functional traits are morphological, physiological, or phenological features – measurable at the individual level - affecting fitness (Violle et al., 2007). Measuring mechanistic traits at the individual (and even species) level in natural communities is rather impossible. Morphological traits that reflect mechanistic traits are traditionally used in phytoplankton ecology (Litchman & Klausmeier, 2008), and often result in the use of some key traits, such as cell size and organization. Morphological traits also enable classifying phytoplankton taxa into ecological groups (Salmaso et al., 2015), which can help better relate ecosystem functioning to community diversity (Abonyi et al., 2018a). Grouping species into ecological, often called 'functional groups', is increasingly adopted by ecologists (Nock et al., 2016). A frequently used functional approach is the classification *sensu* Reynolds (FG) based on habitat templates (Reynolds et al., 2002), which has been advocated as a trait-based approach (Kruk et al., 2021); although we still need to get a mechanistic understanding to link ecosystem-level processes to community composition based on FGs (Abonyi et al., 2021).

At the scale of hydrodynamic events, short and long responses can be expected with a modification in phytoplankton species composition and dominance, and a corresponding alteration in functional trait composition. Short-term dynamics in water discharge should promote larger biodiversity in river phytoplankton, partly explained by meroplankton. A bi-monthly sampling in the Moselle river already demonstrated that diversity and the composition of phytoplankton assemblages are clearly linked to river discharge (Descy, 1993).

5

The Loire River is one of the four largest Atlantic rivers with 200-300 m of width in its lower sections and about 1,012 km of length from its source to the estuarine zone (Moatar et al., 2022). Phytoplankton from the Loire have been widely studied since 1920, but its short-term dynamics have never been shown. Many efforts have been conducted since 1991 to limit anthropogenic phosphorus point sources in the hydrosystem to counteract eutrophication which was reaching some extreme levels in the 1980s with chlorophyll-a concentration often over 250 µg L^{-1} (Moatar & Meybeck, 2005; Minaudo et al., 2015). Over time, the phosphorus concentration dropped by a factor of three and the Loire phytoplankton now seem to be highly P-limited in late summer (Oudin et al., 2009; Floury et al., 2012; Minaudo et al., 2015, 2018, 2021). Longitudinal changes in functional composition, coinciding with the main hydro-ecoregions, have been highlighted, and associated with regional differences in the N:P and Si:P ratios (Abonyi et al., 2014). The Loire River phytoplankton have three distinct assemblage types, upstream detached benthic pennate diatoms, planktic centric diatoms in the middle section (in accordance with an increase in water residence time) and coccal green algae together with small centric diatoms downstream (in accordance with shallowness and increased light availability) (Abonyi et al., 2012; Descy et al., 2012). The Middle Loire River (465 to 772 river km from the headwaters) combines most of the conditions that may favour both pelagic and benthic growth: high light availability with low water level in summer (≈1m), high water temperature (Seyedhashemi et al., 2022) and a river morphology with multiple channels, adjacent pools, and numerous islands, slowing down the flow velocity (Latapie et al., 2014). The Middle Loire receives 40% of the total basin contribution, with very little amount of lateral water inputs, making this section the most representative of the large lowland Loire River. Based on the presence of true planktic species (centric diatoms), one can say that autogenic process dominates from the Middle Loire, which makes it an excellent site to study short-term dynamics. A single station was chosen in the Middle Loire and its short-term temporal dynamics were analysed over two hydrological summers in 2013 and 2014. Based on an every 3-day sampling frequency, the short-term variations in river discharge were related to the variations in both local physical and chemical parameters and phytoplankton assemblages.

The objective of this study was (1) to highlight the changes in physical, chemical and biological parameters associated with water discharge increase (even in low amplitude), (2) to identify short-term

6

response of phytoplankton assemblage and characterize key taxa and their traits, (3) to highlight a potential effect of repeated disturbances on phytoplankton assemblage, and (4) to evaluate the role of meroplanktic algae on phytoplankton diversity in connection with the benthic retention hypothesis. Studies combining the monitoring of water quality variables (nutrients, physical and chemical parameters) with community data on phytoplankton at a near-daily scale remain scarce.

Method

Study area and sampling location

The geographical and physical characteristics of the Loire River basin have formerly been described extensively in the literature (Descy et al., 2009; Moatar et al., 2022). The sampling station, located at Cinq-Mars-La-Pile near Tours in France, is considered representative of the Middle-Loire (Minaudo et al., 2015). It covers 40 % (43.6 $x10^3$ km^2) of the total basin contribution with an annual mean river discharge ~355 m^3 s^{-1}. The Loire River does not receive any significant inflow over 272 km upstream before arriving to Cinq-Mars-La-Pile, except some groundwater inputs from the Beauce aquifers under high agricultural pressure (Lalot et al., 2015).

Daily river discharge and physical and chemical data

Daily river discharge (Q) at gauging station was downloaded from the online open national water monitoring database (http://www.hydro.eaufrance.fr/). Water temperature, pH, dissolved oxygen and conductivity were monitored hourly by Electricité de France (EDF), upstream of the Avoine nuclear power plant, 20 km downstream from our sampling site. Global solar radiation originated from SAFRAN dataset re-analysis (Quintana-Segui et al., 2008), and were averaged over the previous week to account for prior conditions that might had impacted phytoplankton at a given date (Várbíró et al., 2018).

Sampling design

Water was sampled at the thalweg from a bridge in the main river channel. Total suspended solid concentrations (SM) were measured every day. The following parameters were analyzed on a 3-day frequency basis from November 2011 to October 2014: dissolved and particulate organic carbon (DOC and POC), total and dissolved inorganic phosphorus (TP and DIP), total nitrogen (TN), total dissolved

7

193 nitrogen (TDN) and nitrates ($N\text{-}NO_3^-$), dissolved silicon (DSi), chlorophyll-a and pheopigment
194 concentrations. Filtrations were immediately made on-site with 0.45 µm cellulose acetate membrane
195 filters for chemical parameters and with 0.70 µm glass filter (Whatman GFF) previously burned at
196 500°C during 6 hours for chlorophyll-a and pheopigment. SM was determined by filtration of a precise
197 volume of each water sample through pre-weighed filters and by drying them at 105°C. After filtration,
198 water samples and filters were stored at -80°C in polypropylene tubes after acidification of aliquots for
199 nitrates, DIP and DOC analysis. Tubes and filters were unfrozen the day of the analysis. Dissolved
200 organic carbon, TN and TDN concentrations were measured with a carbon and nitrogen analyzer
201 (Shimadzu TOC-V CSH/CSN with TN unit) according to standard protocols from manufacturer
202 (Shimadzu TOC-VCSH/CSN User Manual). Nitrates concentration was determined by ionic
203 chromatography. Phosphorus was measured by colorimetry after solid digestion (potassium-persulfate
204 digestion) when measuring TP (Grasshoff et al., 1983). Dissolved silicon was measured by colorimetry
205 (Aminot & Kérouel, 2004). For POC analyses, the filters were first treated with HCl 2N to remove
206 carbonates, dried at 60°C for 24 hours and then measured with a C/S analyzer (LECO C-S 200).
207 Chlorophyll-a (Chl-a) and pheopigment were measured by fluorimetry at a wavelength > 665 nm after
208 an excitation step between 340 and 550 nm (Strickland & Parsons, 1972). To estimate living
209 phytoplankton and meroplankton in terms photosynthetic activity, we calculated the particulate organic
210 carbon to chlorophyll-a ratio (POC:chl-a) for each sample. It is used as an indicator for ecological and
211 physiological state of phytoplankton, with low ratio when particulate organic matter is dominated by
212 living phytoplankton and high values when there is a lot of organic dead materials (Bibi et al., 2020).
213 Phytoplankton were collected from April to October, with 12 samples in 2012, 44 in 2013 and 44 in
214 2014. Phytoplankton community composition was only related to hydrology in summers 2013 and 2014,
215 where samples were taken with an even distribution (i.e. every 3 days). Summers 2013 and 2014
216 represented ~20 samples in total for each year. Phytoplankton samples were fixed on-site after sampling
217 with Lugol solution. Phytoplankton species were identified with an inverted microscope according to
218 the Utermöhl method (Utermöhl, 1958). Phytoplankton manuals for species identification were Geitler
219 (1930-1932), Huber-Pestalozzi (1955), Fott (1968), Ettl et al. (1978, 1985), Komárek and Fott (1983),
220 Starmach (1985), Popovský and Pfiester (1990), Komárek and Anagnostidis (1999, 2005). If centric

8

diatom dominance appeared, we prepared permanent slides following the Comité Européen de Normalisation (2003) standard. Diatoms were identified using Krammer and Lange-Bertalot (1986, 1988, 1991a, 1991b, Lange-Bertalot (2001) and Krammer (2002). The phytoplankton concentration was first approximated in cells mL^{-1}, and then expressed as wet-weight biomass (mg L^{-1}) using species-specific biovolumes obtained by geometrical approximation according to (Lund & Talling, 1957; Rott, 1981). We converted wet weight biomass into carbon biomass (mgC L^{-1}) based on Eppley et al. (1970). Phytoplankton species were assigned to Reynolds functional groups (RFG) according to Borics et al. (Borics et al., 2007), Padisák et al. (2009), and Abonyi et al. (2021). We quantified the dominance relationships based on the inversed Simpson using the *diversity* function of the 'vegan' library in R (Oksanen, 2013).

Identification of hydrological events and associated periods

During monitoring of river discharge, a river flow peak was identified when the daily river flow F increased rapidly over a few days, *i.e.* when the slope dF/dt became positive between two consecutive days. This is noticed as * on Fig. 1. The use of the daily average flow rate allows to smooth the curve, but it is possible to perform a smoothing over a few days if the inter-day variations are too big. Minor peaks (even small as 5 $m^3 s^{-1} day^{-1}$) were also identified when a slight increase in flow (even over two days) was coupled with changes in biochemical parameters such as POC:chl-a ratio.

To highlight change in phytoplankton assemblage associated with hydrological events, we identified different periods according to their timing before and after peak flow events (Fig. 1). The 'After' period begins when water discharge start increasing (t*). 'Before' and 'After' thus correspond to the increase and the beginning of the decrease in water discharge, respectively. It ends at the end of the recession curve of the river flow at t_2 (Fig. 1). We termed periods outside 'Before' and 'After' 'Stable'.

We then tested if these periods corresponded to distinct phytoplankton assemblages through multivariate analyses, for each year independently. Three assemblages per year were highlighted, called 'stable' assemblages (during stable periods), 'disturbed' assemblages (from t* to t_2) and 'repeatedly disturbed' assemblages (at least two successive disturbed periods).

Multivariate analysis

9

About 150 phytoplankton species have been observed with many rare species. To characterize the short-term relationships between environmental variables (explanatory variables) and taxa biomass (response matrix), a canonical correspondence analysis (CCA) (Legendre & Anderson, 1999) has been performed for each year, using 'ade4' and 'vegan' R libraries (Oksanen, 2013). This method is based on both multiple regression and ordination methods. Prior to these canonical analysis, phytoplankton (biomass) community data were Hellinger-transformed to remove the effects of both rare (many zeros) and dominant taxa (Legendre & Gallagher, 2001). The environmental parameters were centered and scaled and collinearity was checked. The link between explanatory and responses variables was tested through a Monte Carlo permutation test with 999 replications (Blanchet et al., 2008) using CCA. CCA was used to identify characteristic phytoplankton assemblages associated with hydrological forcing and to identify environmental parameters. A taxa contributes to a canonical axis if its variability in relative frequency among samples contributes to the variability of the assemblage.

A correspondence analysis (CA) has also been performed on Hellinger-transformed RFG biomass. A discriminant analysis (DA) was performed on the CA with the function *discrimin* to identify RFG associated with 'stable', 'disturbed' and 'repeatedly disturbed' assemblages. Instead of maximizing the total variance carried by axes 1 and 2 as in a classical CA or CCA, the analysis focused on maximizing the explained inter-group variance depending on a discriminating factor. The level of significance of the discriminating factor has been tested by a Monte Carlo permutation test (based on 999 permutations). All analyses were performed with 'ade4' library in Rstudio.

To link individually taxa and RFG with environmental parameters, a Pearson's correlation matrix was performed with the R library 'corrplot' (Wei & Simko, 2017).

Results

Overall variability of hydrology, physical and chemical parameters and phytoplankton assemblage among years

Hydrology was contrasting among studied years, with water discharges ranging from 50 to 1,900 $m^3 s^{-1}$ (Fig. S1), and up to 3,580 $m^3 s^{-1}$ downstream. The winter high-flow periods in 2013 and 2014 were

10

wet, with a seasonal maximum of 1900 and 1400 $m^3 s^{-1}$, respectively. Minimum summer discharge was 110 $m^3 s^{-1}$ in 2013 and 90 $m^3 s^{-1}$ in 2014. Total suspended solids (SM) concentrations ranged between 0.2 and 137 mg L^{-1}. SM was in general higher in winter due to major hydrological events, though it was also relatively high (≈ 50 mg L^{-1}) in summer during hydrological events. Nitrates concentration was highly seasonal and synchronous with discharge. DSi showed the lowest values between April and June with 1.4 and 1.1 mg SiO_2 L^{-1} in 2013 and 2014, while P-DIP was lowest in July and August, with less than 1 µg P L^{-1} (Fig. S1). Chlorophyll-a values indicated some extensive phytoplankton growth periods, with similar maximum values every year near 60 µg L^{-1}. Centric diatoms systematically dominated the phytoplankton assemblage in spring and then decreased in dominance towards summer, when green algae started to grow (Fig. S1). Phytoplankton at the end of the summer were either dominated by green algae (2012) or diatoms (2013 and 2014).

Physical and chemical parameters in summer 2013

From early July to early September 2013, three discharge peak events with increasing intensity were observed, more than eight days apart (events number 1 to 3, Fig. 2a). SM content increased simultaneously with river discharge, each time with an increasing intensity, consistent with the dynamic of river discharge (Fig. 2b). The third event resulted in a sharp increase in the POC:chl-a ratio of SM in the river, which increased by a factor of 9, whereas this ratio did not fluctuate during the first two events (Fig. 2a). This sharp increase was partly related to the drop of chlorophyll-a concentration in the water (Fig. 2e). Three days after this event, DIP exceeded 40 µg P L^{-1} (Fig. 2c). On 19/08/2013, six days after this third discharge event, DIP decreased to near pre-disturbance values (3 µg P L^{-1}), while chlorophyll-a increased to its pre-disturbance maximum value (44.2 µg L^{-1}). It is noteworthy that overall, DIP and chlorophyll-a concentration correlated negatively (Pearson's correlation, $r = -0.57$; $p = 0.003$), indicating DIP consumption when phytoplankton biomass was high. DOC increased steadily over 9 days following the third discharge event (Fig. 2d). A slight increase in DOC was also observed on 04/08/2013, following event 2. Phaeopigment concentration remained unchanged by the discharge events.

A minor increase of river discharge could also be observed at the end of the period, on 03/09/2013 (number 4, Fig. 2a). This event doubled the POC:chl-a ratio of suspended matter in the river and led to

11

a 50% increase in DOC (Fig. 2d). Two 'stable' periods (outside the before/after periods) could be identified during the summer 2013.

The inverse Simpson index increased during stable hydrology periods, and decreased during peak discharge events (Fig. 2f). The strongest event 3 resulted in the minimum value of the index, with 2.3 on 19/08/2013.

Short-term responses of phytoplankton to hydrology in summer 2013

To characterize the changes in assemblages and relate them to physical and chemical parameters (temperature, pH, oxygen, nutrients, discharge, DOC), a CCA was performed on the biovolumes data (Fig. 3). Environmental variables explained 62.7% of the total variance in phytoplankton community. The sampling dates grouped together following the hydrological periods specified above (Fig. 2). While some periods showed overlaps (e.g. Before1, After3 and Stable2), others remained highly separated along with axis 1 and axis 2 (Fig. 3c).

Along axis 1 of the CCA the consecutive periods Stable1 and Before2, on the right of the axis, contrasted with the initial assembly (Before1) and the ones after event 3 (After3, Stable2 and After4). After1 and After2 had similar 'mean' assemblages, i.e. they were located in the centre of the ordination. Temperature was the most significant variable correlating positively with axis 1 ($r = 0.87$), while nitrates ($r = -0.53$), DIP ($r = -0.41$) and DOC ($r = -0.43$) correlated negatively along with the same gradient (Fig. 3b). Considering the weight of these parameters in the prediction of taxa biomass (i.e. the canonical coefficients of environmental parameters in the CCA), temperature changes had a weight more than twice that of nitrates (-0.17 vs. +0.40) and four times that DIP (-0.09 vs. +0.4). Stable1 and Before2 were characterized by higher water temperatures, but lower concentrations of nitrates, DIP and DOC compared to the other periods. Stable2, Before1, After3 and After4 had higher concentrations and lower water temperature. Along axis 2 of the CCA, After4 was separated from the other periods (Fig. 3c). pH ($r = 0.61$) and temperature ($r= 0.40$), with respective weights of +0.33 and +0.22 were the main variables explaining these differences. After4, which corresponded to the assembly of minor event 4, was thus characterized by lower temperatures and pH.

The most important contributing taxa along with the canonical axes could be separated into three assemblages (Fig. 3a). Assemblage A1 (Fig. 3a), which included the initial assemblage, was

12

characterized by a higher biomass of the diatoms *Skeletonema potamos* (Weber) Hasle (14.4% of contribution to axis 1 and 13.1% to axis 2), centric diatoms (9.0% to axis 1 and 1. 6% to axis 2) and *Nitzschia acicularis* (Kützing) W.M. Smith (4.77% to axis 1), and the green algae *Chlamydomonas* sp. Ehrenberg (8.0% to axis 1 and 3.7% to axis 2), *Coelastrum microporum* Nägeli (1.2% to axis 1 and 2.0% to axis 2) and *Kirchneriella* spp. (1.8% of axis 2 with *K. contorta* (Schmidle) Bohlin, *K. obesa* (W. West) Schmidle and *K. irregularis* (GM Smith) Korshikov). Assemblage A2, corresponding to the Stable1 and Before2 periods, showed higher biomasses of the green algae *Actinastrum hantzschii* Lagerheim (10.4% to axis1), *Crucigenia lauterbornii* (Schmidle) Schmidle (10.7% to axis 1), *Treubaria triappendiculata* Bernard (6. 6% to axis1), *Golenkinia radiata* Chodat (3.9% to axis1), *Lobomonas ampla* Pascher (3.6% to axis1), *Dictyosphaerium pulchellum* Wood (4.4% to axis1), *Oocystis* spp. Nägeli ex A.Braun (2.6% to axis1), and *Didymocystis* spp. (2.7% to axis1 with *D. fina* Komárek, *D. bicellularis* (Chodat) Komárek and *D. planctonica* Korshikov). Assemblage A3 corresponds to After4, with a higher biomass of the benthic diatom *Diatoma vulgaris* Bory (4.1% to axis 1 and 36.7% to axis 2) and *Scenedesmus* spp.: *S.* spp. 3 Meyen with for instance *S.* group *Scenedesmus sensu stricto sensu* Komárek & Fott (3% to axis 1 and 12.7% to axis 2), *S.* spp.1 Meyen with for instance *S.* group *Abundantes / Spinosi sensu* Komárek & Fott (7.8% to axis 2), *Acutodesmus* spp. (Hegewald) Tsarenko (5% to axis 2), *Desmodesmus* spp. (R. Chodat) S.S. An, T. Friedl & E. Hegewald (4.5% to axis 2) and *S.* spp. 2 Meyen with for instance *S.* group *Armati sensu* Komárek & Fott (2% to axis 2). The benthic cyanobacterium *Merismopedia* spp. also contributed to axis 2 (1.16% with *M. glauca* (Ehrenberg) Kützing and *M. tenuissima* Lemmermann). This event-driven short-term succession was also found in the time series of species biomasses (Fig. 4). *S. potamos* (Fig. 4b) and *Chlamydomonas* sp. (Fig. 4c) were positively correlated (Pearson's correlation, $r = 0.52$; $p = 0.008$), with higher biomasses in before1, after2, after3 and stable2 (assemblage 1). In contrast, *G. radiata* (Fig. 4d) and *A. hantzschii* (Fig. 4e), also correlated with each other (Pearson's correlation, $r = 0.62$; $p < 0.001$), and were almost only present during stable1 and Before2 (assemblage A2), i.e. during the period of the lowest discharge fluctuation (Fig. 2a). *D. vulgaris* (Fig. 4g) showed an increase in biomass at the end of the period (After4), as do *Scenedesmus* spp. that are previously punctually present (Fig. 4f).

13

Physical and chemical parameters in summer 2014

The 2014 study period began with a long stable period in terms of discharge, followed by four temporally close discharge peak events, with Q successively peaking on 16/07/2014, 27/07/2014, 9/08/2014 and 15/08/2014, preventing a return to initial conditions (Fig. 5a). The first discharge event started with a gradual increase on 05/07/2014 (100 $m^3 s^{-1}$) and accelerated on 10/07/2014 (210 $m^3 s^{-1}$) to reach a maximum on 16/07/2014 (402 $m^3 s^{-1}$), corresponding to the highest peak of SM observed over summer 2014 with a concentration of 55 mg L^{-1} (Fig. 5b). The following events 3 and 4 resulted in slight increases in SM. A peak in POC:chl-a was observed on 06/07/2014, mainly due to the decrease in chlorophyll-a concentration, potentially indicating an early effect of the first disturbance (Fig. 5e). We considered this period to be isolated from the initially stable period and referred to as Before1.

Event 1 was therefore the major event of summer 2014. It corresponded with a peak of DIP (37 µg P L^{-1}), which continued to increase with the following discharge disturbances up to 60 µg P L^{-1}, reached on 9/08/2014 (Fig. 5c). DOC increased after event 1, with a doubling of its concentration from 2 to 4 mg C L^{-1}, and then remained above 3 mg L^{-1} during the subsequent events (Fig. 5d). When data from both 2013 and 2014 were taken into account, river discharge correlated positively with DOC concentration (Pearson's correlation, $r = 0.62$; $p < 0.001$) and SM (Pearson's correlation, $r = 0.71$; $p < 0.001$).

Chlorophyll-a concentration showed a decreasing trend during the first (Stable) period from 35 to 25 µg L^{-1} (Fig. 5e), likely due to depleted phosphorus availability (Fig. 5c). Chlorophyll-a peaked after event 2 (48 µg L^{-1}) and then remained under 20 µg L^{-1} until the end of the summer. Water discharge events as disturbances decreased chlorophyll-a concentration and increased DIP concentrations. Similarly to 2013, a significant negative correlation between chlorophyll-a and DIP was observed (Pearson's correlation, $r = -0.65$; $p < 0.001$).

Diversity of the phytoplankton assemblage, monitored with the inverse Simpson index, was maximal during the stable period (Fig. 5f), despite declining biomass and limiting dissolved inorganic phosphorus concentrations. Diversity gradually increased again at the end of the disturbed period.

14

Seven periods could be delineated based on the variations in physical and chemical parameters described above (Fig. 5).

Short-term responses of phytoplankton to hydrology in summer 2014

Environmental variables explained 42.6% of variance in the phytoplankton community in 2014 (Fig. 6). pH was removed from the CCA to respect the rule of low collinearity between explanatory variables. Axis 1 was positively correlated with discharge Q (r = 0.88), DIP (r = 0.78), DOC (r = 0.71), silicon (r = 0.60) and SM (r = 0.55) and negatively correlated with nitrates (r = - 0.65) and DO (r = - 0.57) (Fig. 6b). DOC was the parameter with the highest weight (canonical coefficients), with a weight of +0.22, followed by nitrates (- 0.19) and DSi (+0.17). Axis 2 was correlated with SM (r = 0.59), temperature (r = 0.45) and DO (r = - 0.34).

The CCA performed on the 2014 taxa biomass data separated the Stable period to the left of the ordination from the other periods, including Before1, the first pre-disturbed period (Fig. 6c). Axis 2, meanwhile, separated periods chronologically, with After1 at the top right of the ordination, After2, After3 and Before2 in the middle and After4 at the bottom. The post-disturbance assemblages (After1, 2/3 and 4) were thus located in the periphery, while the two transitional assemblages (Before1 and 2) were found near the centre of the ordination, indicating an average composition.

The phytoplankton taxa contributing the most significantly to the canonical axes clustered around 3 assemblages along axes 1 and 2 (Fig. 6a). Assemblage B1 corresponded to the initial assemblage (Stable), with a higher biovolume of diversified green algae: *A. hantzschii* (8.4% to axis1), *D. pulchellum* (6.5% to axis 1), *Dictyosphaerium* sp. Nägeli (5.4% to axis 1 and 6% to axis 2), *C. lauterbornii* (5.8% to axis 1 and 3.4% to axis 2), *Micractinium pusillum* Fresenius (6.2% to axis 1), *Plagioselmis nannoplanctica* (H. Skuja) G. Novarino, I.A.N. Lucas & S. Morrall (3.1% to axis 1), *G. radiata* (2.9% to axis 1 and 2.3% to axis 2), *Actinastrum aciculare* Playfair (2.3% to axis 1 and 4.1% to axis 2), *Monoraphidium* spp. (2.5% to axis 1 with *M. arcuatum* (Korshikov) Hindák, *M. circinale* (Nygaard) Nygaard, *M. contortum* (Thuret) Komárková-Legnerová, *M. griffithii* (Berkeley) Komárková-Legnerová, and *M. tortile* (West & G.S.West) Komárková-Legnerová), *Acutodesmus* spp. (2.3% to axis 1 and 11.3% to axis 2), *Franceia ovalis* (France) Lemmermann (1.3% to axis 1). Only one diatom contributed to the assemblage 1, with *N. acicularis* (3.1% to axis 1 and 5.2% to axis 2).

15

Assemblage B2 associated with the period following the first major disturbance (After1) was characterized by an increase in *Tetraedron* spp. (3.3% to axis 2, with *T. caudatum* (Corda) Hansgirg, *T. incus* (Teiling) G.M. Smith and *T. minimum* (A.Braun) Hansgirg), small indeterminate flagellates (1.8% to axis 2), *Acutodesmus* spp. (11.3% to axis 2), and *Scenedesmus* spp. 1 (4.2% to axis 1 and 5.5% to axis 2). This B2 assemblage was also characterized by decreasing biovolumes of the diatom *N. acicularis* (3.1% to axis 1 and 5.2% to axis 2), and the green algae *Dictyosphaerium subsolitarium* Van Goor (6.1% to axis 2), *C. microporum* (4.5% to axis 2), *A. aciculare* (2.3% to axis 1 and 4.1% to axis 2), and *Chroococcus* sp. Nägeli (5.1% to axis 2). Assemblage B3 observed at the end of the disturbed period (After4) was characterized by a higher biovolume of the benthic cyanobacterium *Merismopedia* spp. (9.6% to axis 1 and 3.3% to axis 2), the diatom *S. potamos* (25.3% to axis 1 and 5.0% to axis 2) and the green algae *Scenedesmus* spp. 3 (3.1% to axis 1).

This succession with a calm period in terms of river discharge, followed by a period with several discharge events was observed in the time series of species biovolumes (Fig. 7), with a bell-shaped curve of colonial green algae during the stable period (Fig. 7a and b). *Tetraedron* spp., a small green alga, although remaining in low biomass, was only observed during the transition period (Fig. 7c). Some genera such as *Scenedesmus* also took advantage of this transition period (Fig. 7f). The benthic cyanobacteria *Merismopedia* spp. and the diatoms *S. potamos* and *N. acicularis* increased temporarily following the major first disturbance (Fig. 7d, e and g).

Phytoplankton assemblage and functional trait compositions between hydrologically contrasting summers

Six characteristic phytoplankton assemblages were identified in 2013 (Fig. 3a) and 2014 (Fig. 6a). We could group them in pairs based on their location in relation to the river discharge disturbances (Fig. 8): two were in stable condition (A2 and B1 grouped as stable assemblage), two following a strong disturbance (A1 and B2, grouped as disturbed assemblage) and two after a series of disturbances, called here ‘repeatedly disturbed’ assemblage (A3 and B3). Common species could be identified with at least four green algae during stable conditions (*A. hantzschii*, *D. pulchellum*, *C. lauterbornii*, *G. radiata*) and one benthic cyanobacterium genus in the repeatedly disturbed period (*Merismopedia* spp.) (Fig. 8). Some diatoms were observed over two periods, such as the needle-shaped species *N.*

16

acicularis during stable and disturbed periods, and the flexible filaments of *S. potamos* during disturbed and repeatedly disturbed periods. Several *Scenedesmus* taxa were observed in the samples, in particular in the repeatedly disturbed periods, in B1 and B2, but the specificity of the species to a period was less markable.

Three typical assemblages of the Loire River could thus be specified here (Fig. 8):

1) The 'stable' assemblage occurred each time in phosphorus-depleted condition, with a diverse assemblage, but under the dominance of colonial green algae and diatoms. The stable assembly could be characterized by 16 species: four species have spine-like morphology (n°5 *G. radiata;* n°8 *F. ovalis;* n°12 *M. pusillum ;* n°13 *T. triappendiculata*), six species are colonial green algae (n°2 *D. pulchellum;* n°3 *Tetrastrum triangulare* (Chodat) Komárek*;* n°4 *A. hantzschii* and *A. aciculare*; n°11 *Oocystis* spp. ; n°12 *M. pusillum ;* n°14 *Scenedesmus* spp., *Desmodesmus* spp. and *Acutodesmus* spp. and two are mobile, with two flagella per cell (n°7 *L. ampla;* n°9 *P. nannoplanctica*). Even if several species were colonial, their size was rather medium compared to large colonial cyanobacteria or Pennate diatoms. The single diatom taxon that regularly occurred during the stable phase was the needle-shaped *N. acicularis*. One third of the 'stable' group species belonged to the co-occurring functional groups **F** and **J**, which correspond to middle and lower sections of large rivers and indicate low turbulence with enhanced residence time and light availability (Abonyi et al., 2021). Finally, these 16 taxa observed in stable conditions belonged to only 5 Reynolds FGs (**D**, **F**, **J**, **X1**, and **X2**).
2) The 'disturbed' assemblage contained 10 taxa, observed either during A1 or during B2. Three species were colonial green algae (n°15 *Kirchneriella* spp., n°14 *Scenedesmus* spp. and n°16 *C. microporum*) and one was mobile, with two flagella per cell (n° 18 *Chlamydomonas*). The flexible filaments of *S. potamos* (n°19) were also observed. The needle-shaped *N. acicularis* (n°1) already observed during Stable period showed a contrasting response to disturbance, with an increase during A1 and a decrease during B2. The group **J** of Reynolds was still the dominant functional group. The characteristic taxa of the 'disturbed' assemblages also

17

belonged to four Reynolds FGs (**D**, **F**, **J**, **X2**, thus loosing **X1** compared with the 'Stable' assemblage).

3) The 'repeatedly disturbed' assemblage had only four characteristic taxa, but all representing different Reynolds FGs (still **D** and **J**, with $\mathbf{T_B}$ and **Lo** more; Fig. 8). The flexible filaments of *S. acicularis* (FG **D**) were still observed. The benthic cyanobacterium *Merismopedia* spp. (n°20), specific of that period, was observed during both A3 and B3 and was the only representative of the group **Lo**. A new benthic diatom was observed, *D. vulgaris* (n°21 ; FG $\mathbf{T_B}$). Finally, half of the four species were benthic, half were diatoms and only one a small colonial green (*Scenedesmus* spp., FG **J**).

The discriminant analysis (DA) performed on the CA of RFG biomass shows that 19% of total variance of the RFG data was explained by three assemblages' types (Fig. 9). The DA separated the stable period on the left from the disturbed period on the upper right and the repeatedly disturbed period on the lower right of the plot (Fig. 9). The FG **F** (cov. -0.83 with axis 1; clear epilimnetic habitat) and **X1** (cov. -0.79; shallow mixed layer in enriched conditions) characterized the stable assemblage. The FG $\mathbf{T_B}$ (cov. 0.55 with axis 1; highly lotic environments, streams and rivulets) characterized both disturbed and repeatedly disturbed assemblages. The FG **D** pointing to the upper right (covariance of 0.55 with axis 1 and 0.32 with axis 2 ; shallow enriched turbid water including rivers) characterized the disturbed assemblage. The FG **Lo** pointing to the lower right (cov. -0.77 with axis 2; summer epilimnion) characterized the repeatedly disturbed period.

Most RFG and taxa positively correlated with water temperature and solar radiations, while they negatively correlated with river discharge and DIP, irrespective of life form and taxonomic position (diatoms, benthic taxa or colonial green algae, Fig. 10). Chlorophyceae biomass thus correlated positively with solar radiation (Pearson's correlation, $r=0.30$; $p=<0.01$) and negatively with river discharge (Pearson's correlation, $r=-0.30$; $p<0.01$). Only the benthic diatom *D. vulgaris* correlated negatively with temperature, and positively with nitrates.

Variance partitioning showed that time generally explained a low proportion of total variance in phytoplankton, with less than 5% (except the 22% for *Chlamydomonas* sp. in summer 2013; see **X1** on Fig. S2). DIP concentration explained between 10 and 40% of the variance at both the seasonal and

18

short-term time scale for centric diatoms and *N. acicularis* (codon **D** – see **X3** on Fig. S2). Interestingly, water temperature appeared as the most significant predictor for many taxa if data were pooled, but also when analysed separately (see **X2** on Fig. S2).

Discussion

Here, we asked how short-term alterations in water discharge affected the physical and chemical environment and corresponding changes in phytoplankton community composition and diversity in the Middle Loire. In two contrasting summers, our data suggested that hydrological events systematically affected phytoplankton composition, along with three assembly types: a stable assemblage type with many colonial green algae; a disturbed assemblage type that decreased in biomass but benefited from new taxa such as *S. potamos* ; and a repeatedly disturbed assemblage type that benefited from the resuspension of benthic species, temporarily replacing colonial greens. These short and long responses to disturbance allowed for the maintenance of greater taxonomic and functional diversity on a seasonal scale in the Loire River. Taxa richness is mainly driven by green algae and diatoms in accordance with literature (Wehr & Descy, 1998; Wang et al., 2014). This suggests that community dynamics of phytoplankton are predictable in the Middle section of large rivers, if hydrology and hydrology-related parameters are monitored with high resolution.

The biogeochemical functioning of large rivers differs strongly between high and low flow, the latter corresponding to a growing period for phytoplankton and so represents strong biological activity. Variations in discharge, e.g. "water flush", can occur over a few hours that dilutes phytoplankton biomass, increases the mortality rate, and changes a full set of environmental conditions (e.g. turbulence, light climate, nutrients availability). However, community dynamics in phytoplankton has rarely been studied at a sub-weekly time scale – but chlorophyll-a (Bowes et al., 2016) and community biomass (Pathak et al., 2021) - in response to river hydrology (Istvànovics & Honti, 2011), in particular at a fine-scale taxonomic and functional levels.

Here, we could identify eight water discharge events that have affected the Loire River phytoplankton. Even minor discharge increases modified the physical and chemical parameters with an increase in the

19

525 POC:chl-a *ratio*, a decrease in phytoplankton biomass, and a change in assemblage structure. Pickett
526 and White (1985) defined disturbance as "any relatively discrete event in time that disrupts ecosystem,
527 community, or population structure, and that changes resources, availability of substratum, or the
528 physical environment". The hydrological events thus represented disturbances for the phytoplankton,
529 leading to a dilution of the bulk community but with alterations in community composition based on
530 species functional characteristics before, during, and after disturbance. Wang et al. (2014) highlighted
531 distinct assemblages driven by hydrological forcing in a large subtropical river, with after-flood
532 assemblages associated with higher abundance of green algae and tychoplanktic taxa. While
533 disturbances in rivers are generally associated with high floods, which then mobilize nearby sediments,
534 here, we refer to a disturbance as soon as the river discharge increases even slightly, such as a daily
535 increase of 5 m^3 s^{-1} day^{-1}. Our study highlights that hydrology-related disturbance is not necessarily
536 related to any threshold, rather, the disturbance can even under slight changes in hydrology.
537 The rate of change of the river discharge appears more important than its intensity to constrain the
538 phytoplankton biomass and assemblage in the Loire River. The discharge rate of change with the
539 previous day was overall mainly negative: river discharge decreased compared with the previous day
540 62% of days (all seasons considered), while it increased during 35% of the days or remained stable for
541 3% of the days. When we focused on the period of May to September, river discharge decreased 67%
542 of the days. Hydrological recession thus represents the most common condition in the Middle Loire
543 River in summer.

544 **Short-term changes in physical and chemical parameters**

545 Temperature, solar radiations, nutrients and river discharge have been identified as main drivers of
546 river phytoplankton at the seasonal scale (Descy et al., 2013). We had expected that during summer
547 high temperature influenced less phytoplankton production and assemblages, being already high
548 compared with spring and fall. In summer, mean daily water temperature varies by a few degrees over
549 a few days, following meteorological forcing and high/low pressure events. Water temperature was a
550 stronger predictor for the biomass of individual phytoplankton taxa than solar radiation. Most of the
551 variance in taxa biomass was also explained by water temperature. It is therefore likely that water
552 temperature indirectly affected phytoplankton growth, e.g. jointly with other meteorological

20

553 conditions such as calm and sunny *versus* disturbed periods. River temperature follows a diurnal cycle
554 and a seasonal cycle, associated with meteorological forcing and depending on the hydrological
555 context. Water temperature is sensitive to air temperature, relative humidity, solar radiation and river
556 width, but also river discharge, upstream temperature (Gu & Li, 2002), and lateral groundwater inputs
557 (Wawrzyniak et al., 2017). More than a controlling factor, water temperature seems to be a good proxy
558 for short-term meteorological and hydrological forcings. Changes in the similarity of pelagic diatoms
559 in a large German river have been successfully linked to the antecedent precipitation index, which
560 considers rainfall and wetness of the basin, and so remobilisation on a wider scale (Wu et al., 2016).
561 At the short time scale, CCA showed that DIP and DOC were associated with discharge peak events
562 for both 2013 and 2014, where suspended matter (SM) also increased nearly simultaneously with
563 discharge peaks. In 2014, SM strongly increased just after the first main disturbance, while next
564 events, despite being higher in intensity, did not lead to higher SM concentration. Remobilization of
565 organic and inorganic particles from the benthos in the Middle Loire seems to depend on the delay
566 between discharge disturbances, with a small remobilization if time for settling of suspended particles
567 from one event to the next is too short.
568 In conjunction with peaks in SM, most of the discharge disturbances resulted in simultaneous drops in
569 chlorophyll-a concentration, likely by dilution. It is known that phytoplankton biomass in large rivers
570 varies inversely with discharge, and is linked to water residence time and hydrology-mediated light
571 availability (Wehr & Descy, 1998; Várbíró et al., 2018). However, on our semi-weekly time series, we
572 observe that chlorophyll-a tends to increase rapidly 2-6 days after a discharge event, probably due to
573 both the enrichment by meroplankton and the phytoplankton growth stimulated by the mobilisation of
574 nutrients (Minaudo et al., 2018). The increase of SM in the river recharges phosphorus, by desorption
575 processes from the particulate phase to the dissolved one and diffusion of pore water from the
576 underlying sediment (Reddy et al., 1995). Discharge events in summer also flush DIP-repleted water
577 with direct and diffuse inputs from the upper catchment. Disturbances have, therefore, first a negative
578 impact on the phytoplankton biomass (dilution effect combined with light limitation due to
579 resuspended solids), then a positive impact by recharging the ecosystem in potentially bio-assimilable

21

phosphorus. The response of the assemblages to short-term forcing in P-limited conditions should differ from the response in eutrophic conditions.

Short-term nutrients dynamic in summer can be related here to short-term dynamics in phytoplankton and the uptake of nutrients for its biomass. The summer concentration of DIP was lower than 10 µg P L^{-1} in 50% of the samples, while nitrates concentration, with a minimum concentration of 950 µg N L^{-1}, was sufficient throughout the year for the growth of phytoplankton. A mean biomass of 60 µg L^{-1} (we had 40 to 50 µg L^{-1} during this study) indeed requires ~ 100 µg P L^{-1} (Dillon & Rigler, 1974) and 722 µg N L^{-1}, based on the Redfield ratio. The concentrations of silicon remained also high enough most of the year, with values >1 mg SiO_2 L^{-1} in 99% of samples. The lack of correlations between DSi or nitrates concentrations with the phytoplankton biomass can be explained by the fact that nutrient uptake by phytoplankton remained low compared to the nutrient stock in the river. On the contrary, concentrations of DIP and chlorophyll-a were negatively correlated. Short-term DIP concentration in the Loire River is thus controlled by phytoplanktic uptake, with maximum DIP concentrations reached when chlorophyll-a concentration is minimal. Descy (2012) also observed concentrations <10 µg P L^{-1} from June to October in the Loire River. The molar N:P ratio calculated on biologically available nutrients (Ptacnik et al., 2010) was always > 64 during that study, clearly above the 16:1 Redfield ratio, also confirming that P was a limiting nutrient for growth, in accordance with literature (Minaudo et al., 2015). Over the last 30 years, the Loire River has indeed undergone changes in its phytoplankton assemblages, with a 90% biomass decrease, which has been related to different factors: P reduction, altered discharge and the invasion of the Asian clam *Corbicula* sp. (Minaudo et al., 2021). Planktic cyanobacteria always remained a minor fraction of the total phytoplankton biomass, irrespective of the study period (Descy et al., 2012; Minaudo et al., 2021).

Short-term DOC dynamics were also related to river discharge, with increases of 1 to 5 mg C L^{-1} following discharge disturbances. Most of the total organic carbon (TOC) was in the dissolved form, with DOC representing ~70% of the TOC, in accordance with literature (Peterson et al., 1994) and other stations on the Loire River (Minaudo et al., 2015). The highest DOC concentrations were observed during the main hydrological events, indicating a remobilization of DOC pool during discharge peak events. DOC originates from both terrestrial sources (hydrologically connected soils

22

608 and wetlands) and local production by phytoplankton, microphytobenthos and the microbial loop.
609 Upstream terrestrial DOC inputs thus fuels a semi-labile pool, more conservative, while local
610 production fuels a labile pool, rapidly lost through photolysis, flocculation, consumption or adsorption
611 (Del Giorgio & Pace, 2008). A higher local production or lower lost processes may explain that DOC
612 concentration generally increases after a discharge disturbance. DOC could thus represent an excellent
613 chemical proxy for river discharge disturbances in the Loire River, and also elsewhere.
614 In recent years, the use of *in situ* high-frequency spectrophotometric and electrode technologies,
615 particularly of chlorophyll fluorescence probes, represents a good opportunity to go further in the
616 study of short-term dynamics with time series data at a scale down to the minute (Wade et al., 2012).
617 Thresholds of environmental drivers can be highlighted, as for water discharge and temperature whose
618 thresholds for cyanobacteria blooms could have been calculated in a eutrophic river (Bowes et al.,
619 2016). The main limitation of new technologies is that nutrients are by now rarely measured at such a
620 fine time scale. Moreover, the simultaneous acquisition of assemblage data remains scarce, although
621 sensor development is progressing. The coupling of high frequency physical and chemical
622 measurements with daily monitoring of species by flow cytometry or sequencing for instance would
623 be a real step forward in the near future to increase our understanding of assembly rules and short-term
624 drivers of river phytoplankton.

625 **Short-term functional changes in phytoplankton in response to hydrological disturbance**

626 The phytoplankton assemblage measured semi-weekly was in agreement with the seasonal succession
627 already described in the Loire River (Abonyi et al., 2012, 2014; Descy et al., 2012) and more generally
628 in large rivers, with a spring bloom of diatoms, followed by small centric diatoms in May-June, and by
629 Chlorophyceae during summer (Descy et al., 2012, 2013). Diatoms represented ~10% of the total
630 biomass in summer, which indicates stable low flow conditions that can trigger the sedimentation of
631 large diatoms. It is known that centric diatoms develop successfully in well-mixed, nutrient-replete
632 and turbid rivers, which are not so different from shallow lakes (Reynolds et al., 1994). Here also,
633 small centric diatoms dominated the community over large diatoms when present. Summer coccal
634 green algae, some with ornamentations and/or mucilage, were typical of the summer highly diverse
635 Chlorophyceae assemblage (Descy et al., 2012). Their dominance has been associated to high light

23

and shallow depth as main environmental drivers (Abonyi et al., 2012). Coccal green algae took advantage of stable periods between disturbances, in accordance with the benthic retention hypothesis (Istvànovics & Honti, 2011). Many species of the planktic genera *Scenedesmus*, *Acutodesmus* and *Desmodesmus* were also observed during all periods from stable to repeatedly disturbed periods. These genera are among the commonest green algae and one of the most diverse genera (John et al., 2002), and have already been observed with high biomass in many rivers elsewhere (Gosselain et al., 1994). Their small size and rapid growth rate make these algae very competitive in rivers and water bodies, allowing a good sustainability of populations in high flushing environments where dilution effects are likely. *Scenedesmus* spp. have already been related to hydrological factors and temperature in a German lowland river (Wu et al. 2011). Also, coccal greens represent a group that is favoured by sedimentation and resuspension during hydrological events (Reynolds & Descy, 1996). In nutrient depleted conditions, small cells are also more competitive for nutrients uptake than large ones at low concentrations, thanks to a higher surface/volume ratio. While these taxa are especially sensitive to grazing by zooplankton, top-down effects remain largely understudied in the Loire River (Lair & Reyes-Marchant, 1997), but also elsewhere.

Despite the discharge disturbances, colonial green algae, such as *Kirchneriella* spp. or the coccal *C. microporum*, remained an important part of the total biomass. On the contrary, colonial green algae with spine-like ornamentations decreased and raised the question of a counter-selection driven by the turbulent regime. The presence of spines may be useful against grazing and to regulate sinking velocity. Two main strategies against grazing were observed here (Lürling, 2021), the presence of spines and the colonial form, sometimes mucilaginous. Grazing pressure in large river is, however, less important than in lakes, because zooplankton is dominated by small-sized fast growing species because of flushing (Wehr et al., 2015). However, our knowledge on how long-term changes in hydrology with extended low flow conditions and re-oligotrophication affected zooplankton community composition remains largely elusive. Spines and protuberances can also increase the resistance to sedimentation, by increasing fluid drag coefficient, and stabilization of the horizontal position with the highest form resistance (Padisák et al., 2003). Spines can also increase the effects of

24

663 viscosity at an individual scale like mucilage (Naselli-Flores et al., 2021) and help regulate population
664 density to avoid collapse.
665 *S. potamos*, a filamentous diatom, was also observed in the aftermath of summer discharge
666 disturbances. Cells of *S. potamos* form a chain attached by external tubes organized in one marginal
667 ring, giving flexibility to the filament able to support deformations. The length of the chain depends on
668 river turbulence (Duleba et al., 2014). *S. potamos* is one of the most important species in some
669 eutrophic rivers, with high biomass occurring during the growing season and seems favoured by
670 warmer temperatures and high light availability (Kiss et al., 1994; Abonyi et al., 2018b), including in
671 the Loire River (Descy et al., 2012). It is a warm-stenotherm centric diatom, with a relatively recent
672 dispersion across the World (Duleba et al., 2014), which may make it as a good indicator of late
673 summer warm conditions among planktic river species. Increase in its relative biomass since the last
674 40 years has been observed in the Danube River and was linked to the increase in water temperature
675 (Duleba et al., 2014). This species was also observed by Descy in the Moselle River and related to the
676 stable summer conditions and the minimum discharge (Descy, 1993). This centric diatom has a thin
677 frustule weakly silicified and small chloroplasts. Silicification intensity varies greatly among diatoms
678 and is a strategy against grazing but with a cost on the competition abilities (Assmy et al., 2013;
679 Pančić & Kiørboe, 2018). *S. potamos* is thus competitive for silicon, with an optimal quota two to
680 three times lower than other centric and large diatoms (Descy et al., 2012). Large filament well
681 silicified of *Aulacoseira granulata* (Ehrenberg) Simonsen used to be observed in the Loire River
682 before 1990 when nutrient availability was high, in particular silicon >7 mg L^{-1} (Lair & Reyes-
683 Marchant, 1997). Its cell and filament sizes can also change with turbulence in a large river (Wang et
684 al. 2015). High summer temperature, higher turbulence and low DSi requirement may explain the
685 dominance of *S. potamos* following discharge disturbances in the Loire River. Also, while DSi might
686 not be limiting in most of the European rivers, the Si:P ratio has largely been altered due to P decrease
687 and damming, likely affecting phytoplankton (Abonyi et al., 2014; 2018a).
688 The needle-shaped diatom *N. acicularis* maintained its biomass after the discharge disturbances, and
689 regularly increased in biomass. This truly planktic species is very common in the Loire River and can
690 be abundant at high river discharge (Descy et al., 2012). As shown by experiments and numerical

25

simulations, a needle-like shape can lead to aggregation during sedimentation thanks to hydrodynamic interactions at low Reynolds number, independently on fluid shear and Brownian motion, (Botte et al., 2013). This can be a strategy to decrease sedimentation rate for needle-like shape taxa, such as *Pseudo-nizschia spp.*, which forms chains of needles in stable periods (low Reynolds number), while it becomes individualized in periods of flooding (high Reynolds number) to be more easily driven by turbulent eddies. It would be interesting to make observations of fresh samples of *N. acicularis* in sedimentation to see if this hypothesis is valid for this species. More than minimizing sinking velocity, phytoplankton traits are selected to maximize the entertainability of cells by turbulent eddies (Naselli-Flores et al., 2021). Interestingly, the two main diatoms *N. acicularis* and *S. potamos* belong to both freshwater and marine genera, suggesting a shape that withstands high turbulence as in the sea.

D. vulgaris, a characteristic benthic diatom which normally forms zig-zag colonies attached to the substrate, increased in biomass during repeated discharge events. Living in various habitats in rivers, such as rock and plants, it predominates in eutrophic water with high conductivity and with pH > 7 (Kelly, 2000). This benthic diatom has been observed in high biomass in upstream reaches of the Loire River (Abonyi et al., 2012), but also in the Middle Loire during high flow periods, with other species like *Amphora ovalis* (Kütz.) Kütz. or *Cocconeis placentula* Ehrenberg (Descy et al., 2012). Its presence is, therefore, an excellent indicator of flushing or high discharge events.

Benthic cyanobacteria observed following repeated discharge disturbances were *M. tenuissima* and *M. glauca*. Both meroplanktic species are often associated with bottom silt and live at the water-sediment interface, even if they can be observed in the water column (John et al., 2002). *M. tenuissima* is also indicative of eutrophic conditions, with bottom reducing conditions (John et al., 2002). Already widely observed in the Loire River, it probably develops in the main river channel on the riverbanks (Minaudo et al., 2021). As for cyanobacteria, warm summer temperature may have promoted this species.

Benthic taxa were thus the most responsive group to repeated disturbances, in accordance with their shear-induced resuspension. The presence of benthic diatoms and cyanobacteria with discharge disturbances has already been highlighted in the literature (Rojo et al., 1994; Abonyi et al., 2012). Antecedent discharge disturbance is thus important to consider for the assembly rules of

26

719 phytoplankton, as well as the role of meroplankton in sustaining diversity. The maintenance of
720 functional richness is needed to sustain ecosystem functions, while high taxonomic richness with
721 functional redundancy increases the insurance of the community against disturbances (Naeem, 2008).
722 Other biotic and abiotic factors than discharge may have controlled phytoplankton assemblage during
723 stable periods, such as spatial heterogeneity. It has been shown that the Loire River has a very high
724 taxonomic diversity, partly explained by its relative shallowness, braided arms and 'dead zones'
725 occurring in the Middle and Lower river sections (Descy et al., 2012). Spatial heterogeneity in
726 phytoplankton distribution increases as river discharge decreases. Our sampling station, located in the
727 Middle Loire River, has no significant upstream tributaries over 272 km, but many disconnected pools
728 can form under low flows and may represent a potential inoculum of planktic species. Grazing
729 pressure and selectivity may also have controlled phytoplankton assemblage. Small zooplankton
730 probably developed during stable period of summer months, favoured by low discharge and high
731 temperature, especially because we observed traits against grazing. Such zooplankton data would help
732 increase our understanding of the functional traits of green algae. Mussels, such as the Asian clams
733 *Corbicula* spp., are also known to reduce phytoplankton and meroplankton biomasses in the Loire
734 River (Descy et al., 2012). However, feeding selectivity seems to be low in mussels (Boltovskoy et al.,
735 1995; Frau et al., 2016). One can also consider that *Corbicula* spp. grazing should not change on a
736 short-term scale in response to discharge except if the mixing regime shifts from laminar to turbulent.
737 Mixing regime of the water column is indeed essential to bring phytoplankton cells in contact with
738 benthic invertebrates (Smith et al., 1998).
739 With climate change, summer conditions of high temperatures and strong solar radiations are likely to
740 favor benthic primary producers, while phytoplankton may remain limited by phosphorus availability.
741 Severe low water levels, such as those observed in 2022 in the Loire River, will likely enhance benthic
742 growth, on the other hand, likely decrease exchanges between the benthic and planktic compartments.
743 The decrease of meroplankton enrichment, i.e., taxa that can potentially live both sedimented and
744 resuspended, could compromise the biodiversity of the Loire River. Meroplankton should be
745 emphasized along with the benthic retention hypothesis (Istvànovics & Honti, 2011) and points at the

27

importance of hydrological variations in mediating phytoplankton biodiversity, biomass and ecosystem functioning via resuspension.

Conclusion

This study analyzed the impact of short-term discharge disturbances on physical, chemical and biological parameters and on the Loire River phytoplankton assemblage. Suspended matter increased with river discharge, while chlorophyll-a concentration decreased due to the dilution effect. We highlighted three assemblage types along with increasing hydrological forcing: (i) a short community response associated with the dilution and collapse of community dominance, followed by the enrichment of benthic species. Discharge disturbances promoted species with specific adaptations to turbulence, while stable periods in terms of hydrology promoted species with adaptations against sedimentation and grazing. DIP dynamic was directly linked to its consumption by phytoplankton as it correlated negatively with biomass. Even in the short term, temperature remains a key parameter, which was positively correlated to taxa biomass and is likely an excellent proxy for meteorological and hydrological forcings at the short-term scale. In a context of re-oligotrophication and global warming, meroplanktic algae will likely plays a decisive role in maintaining phytoplankton diversity and ecosystem functioning in the Loire River, which may also likely the case in other shallow and large rivers.

Acknowledgments

The authors are thankful to the water basin authority (Agence de l'Eau Loire Bretagne) for providing long-term water quality data and allowing the publication of phytoplankton data. Authors are also grateful to “Electricité de France” for providing data on continuous water temperature measurements for the Middle Loire River. The authors are thankful to Anne Marie Lançon for phytoplankton identification and to Laurence Lanctin, Yannick Bennet, André Dubois, Hervé Couet and Didier Louvel for their help on the field. AA was supported by the FK 142485 project (National Research, Development and Innovation Office, Hungary) and by the János Bolyai Research Scholarship of the Hungarian Academy of Sciences (2023). We thank Viktória B-Béres and two anonymous referees for helpful comments on an earlier version of the manuscript.

28

Author Contributions

FM, CM and NG collected data on physical and chemical parameters; AA and ML collected data on phytoplankton; AP and CM conceptualized the study, and performed the data analyses and statistics. AP, CM, NG and AA wrote the manuscript, with equal contributions from all authors.

Data Availability Statement

The data presented in this study will be available as Supplementary materials.

Conflicts of Interest

The authors declare no conflict of interest.

29

784 **References**

785 Abonyi, A., Z. Horváth & R. Ptacnik, 2018a. Functional richness outperforms taxonomic richness in
786 predicting ecosystem functioning in natural phytoplankton communities. Freshwater Biology 63: 178–
787 186. https://doi.org/10.1111/fwb.13051

788 Abonyi, A., É. Ács, A. Hidas, I. Grigorszky, G. Várbíró, G. Borics & K. T. Kiss, 2018b. Functional
789 diversity of phytoplankton highlights long-term gradual regime shift in the middle section of the
790 Danube River due to global warming, human impacts and oligotrophication. Freshwater Biology 63:
791 456–472. https://doi.org/10.1111/fwb.13084

792 Abonyi, A., J.-P. Descy, G. Borics & E. Smeti, 2021. From historical backgrounds towards the
793 functional classification of river phytoplankton sensu Colin S. Reynolds: what future merits the
794 approach may hold? Hydrobiologia 848: 131–142. https://doi.org/10.1007/s10750-020-04300-3

795 Abonyi, A., M. Leitao, A. M. Lançon & J. Padisák, 2012. Phytoplankton functional groups as
796 indicators of human impacts along the River Loire (France). Phytoplankton responses to human
797 impacts at different scales. Hydrobiologia. 233–249. https://doi.org/10.1007/s10750-012-1130-0

798 Abonyi, A., M. Leitão, I. Stanković, G. Borics, G. Várbíró & J. Padisák, 2014. A large river (River
799 Loire, France) survey to compare phytoplankton functional approaches: do they display river zones in
800 similar ways? Ecological Indicators 46: 11–22. https://doi.org/10.1016/j.ecolind.2014.05.038

801 Aminot, A. & Kérouel, R., 2004. Hydrologie des écosystèmes marins: paramètres et analyses. Editions
802 Quae. Ed. Ifremer. 336 pp.

803 Assmy, P., V. Smetacek, M. Montresor, C. Klaas, J. Henjes, V. H. Strass, J. M. Arrieta, U. Bathmann,
804 G. M. Berg, E. Breitbarth, B. Cisewski, L. Friedrichs, N. Fuchs, G. J. Herndl, S. Jansen, S. Krägefsky,
805 M. Latasal, I. Peeken, R. Röttgers, R. Scharek, S. E. Schüller, S. Steigenberger, A. Webb, & D. Wolf-
806 Gladrow, 2013. Thick-shelled, grazer-protected diatoms decouple ocean carbon and silicon cycles in
807 the iron-limited Antarctic Circumpolar Current. Proceedings of the National Academy of Sciences.
808 https://doi.org/10.1073/pnas.1309345110

809 Barton, A. D., B. A. Ward, R. G. Williams & M. J. Follows, 2014. The impact of fine-scale turbulence
810 on phytoplankton community structure. Limnology and Oceanography: Fluids and Environments 4:
811 34–49. https://doi.org/10.1215/21573689-2651533

812 Bibi, R., H. Y. Kang, D. Kim, J. Jang, G. K. Kundu, Y. K. Kim & C.-K. Kang, 2020. Dominance of
813 Autochthonous Phytoplankton-Derived Particulate Organic Matter in a Low-Turbidity Temperate
814 Estuarine Embayment, Gwangyang Bay, Korea. Frontiers in Marine Science 7: 580260.
815 https://doi.org/10.3389/fmars.2020.580260

816 Boltovskoy, D., I. Izaguirre & N. Correa, 1995. Feeding selectivity of Corbicula fluminea (Bivalvia)
817 on natural phytoplankton. Hydrobiologia 312: 171–182.

30

Borics, G., G. Várbíró, I. Grigorszky, E. Krasznai, S. Szabó & K. T. Kiss, 2007. A new evaluation technique of potamo-plankton for the assessment of the ecological status of rivers. Large Rivers, 17. Archiv für Hydrobiologie Supplement 161: 465–486. https://doi.org/10.1127/lr/17/2007/466

Bormans, M., P. W. Ford, L. Fabbro & G. Hancock, 2004. Onset and persistence of cyanobacterial blooms in a large impounded tropical river, Australia. Marine and Freshwater Research 55(1): 1-15. https://doi.org/10.1071/MF03045

Botte, V., M. Ribera D'Alcalà & M. Montresor, 2013. Hydrodynamic interactions at low Reynolds number: an overlooked mechanism favouring diatom encounters. Journal of Plankton Research 35: 914–918. https://doi.org/10.1093/plankt/fbt033

Bowes, M. J., M. Loewenthal, D. S. Read, M. G. Hutchins, C. Prudhomme, L. K. Armstrong, S. A. Harman, H. D. Wickham, E. Gozzard & L. Carvalho, 2016. Identifying multiple stressor controls on phytoplankton dynamics in the River Thames (UK) using high-frequency water quality data. Science of The Total Environment 569–570: 1489–1499. https://doi.org/10.1016/j.scitotenv.2016.06.239

Carrick, H. J., F. J. Aldridge & C. L. Schelske, 1993. Wind influences phytoplankton biomass and composition in a shallow, productive lake. Limnology and Oceanography 38: 1179–1192. https://doi.org/10.4319/lo.1993.38.6.1179

Comité Européen de Normalisation, 2003. Water quality – Guidance standard for the routine sampling and pre-treatment of benthic diatoms from rivers. European Standard: EN 13946:2003.

Cloern, J. E., 1996. Phytoplankton bloom dynamics in coastal ecosystems: A review with some general lessons from sustained investigation of San Francisco Bay, California. Reviews of Geophysics 34: 127–168. https://doi.org/10.1029/96RG00986

Del Giorgio, P. A. & M. L. Pace, 2008. Relative independence of organic carbon transport and processing in a large temperate river: The Hudson River as both pipe and reactor. Limnology and Oceanography 53: 185–197. https://doi.org/10.4319/lo.2008.53.1.0185

Descy, J.-P., 1993. Ecology of the phytoplankton of the River Moselle: effects of disturbances on community structure and diversity. Hydrobiologia 249: 111–116.

Descy, J.-P., M. Leitao, E. Everbecq, J. S. Smitz & J.-F. Deliege, 2012. Phytoplankton of the River Loire, France: a biodiversity and modelling study. Journal of Plankton Research 34: 120–135. https://doi.org/10.1093/plankt/fbr085

Descy, J.-P., K. Patrick, E. Everbecq, G. Verniers, P. Usseglio-Polatera, P. Gérard, L. Viroux, J. Beisel & J. Smitz, 2009. Continental atlantic rivers. Rivers of Europe. EAWAG/ETH, Switzerland. Elsevier, London 151199.

Descy, J.-P., C. S. Reynolds & J. Padisák, 2013. Phytoplankton in turbid environments: rivers and

31

shallow lakes. Springer Science & Business Media. https://doi.org/10.1007/978-94-017-2670-2

Dillon, P. J. & F. Rigler, 1974. The phosphorus-chlorophyll relationship in lakes 1, 2. Limnology and oceanography 19: 767–773. https://doi.org/10.4319/lo.1974.19.5.0767

Dubelaar, G. B. J., P. J. F. Geerders & R. R. Jonker, 2004. High frequency monitoring reveals phytoplankton dynamics. Journal of Environmental Monitoring 6: 946-952. https://doi.org/10.1039/B409350J

Duleba, M., L. Ector, Z. Horváth, K. T. Kiss, L. F. Molnár, Z. Pohner, Z. Szilagyi, B. Toth, C. F. Vad, G. Várbíró & É. Ács, 2014. Biogeography and phylogenetic position of a warm-stenotherm centric diatom, *Skeletonema potamos* (CI Weber) Hasle and its long-term dynamics in the River Danube. Protist 165: 715–729. https://doi.org/10.1016/j.protis.2014.08.001

Eppley, R. W., F. M. H. Reid & J. D. H. Strickland, 1970. The Ecology of the Plankton Off La Jolla, California, In the period April through September, 1967, Part III, Estimates of Phytoplankton Crop Size, Growth Rate, And Primary Production. ISBN: 0-520-09362-3

Ettl, H., J. Gerloff & H. Hegnig, 1978. Xanthophyceae vol 1. Gustav Fischer Verlag, Stuttgart, 530 pp.

Ettl, H., J. Gerloff & H. Hegnig, 1985. Chrysophyceae und Haptophyceae. Gustav Fischer Verlag, Stuttgart, 515 pp.

Floury, M., C. Delattre, S. J. Ormerod & Y. Souchon, 2012. Global versus local change effects on a large European river. Science of the Total Environment 441: 220–229. https://doi.org/10.1016/j.scitotenv.2012.09.051

Fott, B., 1968. Cryptophyceae, Chloromonadophyceae, Dinophyceae, vol 3. E. Schweizerbart'sche Verlagsbuchhandlung (Nägele u. Obermiller), Stuttgart, 322 pp.

Frau, D., F. R. Molina & G. Mayora, 2016. Feeding selectivity of the invasive mussel Limnoperna fortunei (Dunker, 1857) on a natural phytoplankton assemblage: what really matters? Limnology 17: 47–57. https://doi.org/10.1007/s10201-015-0459-2

Geitler, L., 1930-1932. Cyanophyceae von Europa. Koeltz Scientific Books, Koenigstein, 1196 pp.

Gosselain, V., J.-P. Descy & E. Everbecq, 1994. The phytoplankton community of the River Meuse, Belgium: seasonal dynamics (year 1992) and the possible incidence of zooplankton grazing. Hydrobiologia 289: 179–191.

Grasshoff K, Ehrhardt M & K. Kremling, 1983. Methods of Seawater Analysis. 2nd ed. Verlag Chemie, Weinheim, Germany.

Gu, R. R. & Y. Li, 2002. River temperature sensitivity to hydraulic and meteorological parameters. Journal of Environmental Management 66: 43–56. https://doi.org/10.1006/jema.2002.0565

32

Hiltunen, T., J. Laakso & V. Kaitala, 2006. Interactions between environmental variability and immigration rate control patterns of species diversity. Ecological Modelling 194: 125–131. https://doi.org/10.1016/j.ecolmodel.2005.10.010

Huber-Pestalozzi, G., 1955. Euglenophyceen, vol 4. E. Schweizerbart'sche Verlagsbuchhandlung (Nägele u. Obermiller), Stuttgart, 606 pp.

Istvànovics, V. & M. Honti, 2011. Phytoplankton growth in three rivers: The role of meroplankton and the benthic retention hypothesis. Limnology and Oceanography 56: 1439–1452. https://doi.org/10.4319/lo.2011.56.4.1439

Istvánovics, V., M. Honti, L. Vörös & Z. Kozma, 2010. Phytoplankton dynamics in relation to connectivity, flow dynamics and resource availability—the case of a large, lowland river, the Hungarian Tisza. Hydrobiologia 637: 121–141. https://doi.org/10.1007/s10750-009-9991-6

John, D. M., B. A. Whitton, & A. J. Brook,, 2002. The freshwater algal flora of the British Isles: An identification guide to freshwater and terrestrial algae, University Press, Cambridge. pp. 878.

Johnson, B. L., W. B. Richardson & T. J. Naimo, 1995. Past, present, and future concepts in large river ecology. BioScience 45: 134–141. https://doi.org/10.2307/1312552

Kelly, M., 2000. Identification of common benthic diatoms in rivers. Field Studies Council 9.4: 118 pages.

Kiss, K. T., É. Ács & A. Kovács, 1994. Ecological observations on *Skeletonema potamos* (Weber) Hasle in the River Danube, near Budapest (1991–92, daily investigations). In Descy, J.-P., C. S. Reynolds & J. Padisák (eds), Phytoplankton in turbid environments: rivers and shallow lakes Springer, Dordrecht, Netherlands: 163–170.

Kiss, K. T., A. Schmidt & É. Ács, 1996. Sampling strategies for phytoplankton investigations in a large river (River Danube, Hungary). STUDIA Studentenförderungs GmbH. ISBN 0395000902.

Komárek, J. & B. Fott, 1983. Chlorophyceae, vol 7, Chlorococcales. E. Schweizerbart'sche Verlagsbuchhandlung (Nägele u. Obermiller), Stuttgart, 1044 pp.

Komárek, J. & K. Anagnostidis, 1999. Cyanoprokaryota, vol 1, Chroococcales. Gustav Fischer Verlag, Stuttgart, 548 pp.

Komárek, J. & K. Anagnostidis, 2005. Cyanoprokaryota, vol 2, Oscillatoriales. Gustav Fischer Verlag, Stuttgart, 759 pp.

Krammer, K., 2002. Cymbella. In Lange-Bertalot, H. (ed) Diatoms of Europe. A.R.G. Gantner Verlag

33

915 K. G., Königstein, 586 pp.

916 Krammer, K. & H. Lange-Bertalot, 1986. Bacillariophyceae. 1. Teil: Naviculaceae. Gustav Fischer
917 Verlag, Stuttgart, Stuttgart.

918 Krammer, K. & H. Lange-Bertalot, 1988. Bacillariophyceae. 2. Teil: Bacillariaceae, Epithemiaceae,
919 Surirellaceae. Gustav Fischer Verlag, Stuttgart, Stuttgart.

920 Krammer, K. & H. Lange-Bertalot, 1991a. Bacillariophyceae. 3. Teil: Centrales, Fragilariaceae,
921 Eunotiaceae. Stuttgart.

922 Krammer, K. & H. Lange-Bertalot, 1991b. Bacillariophyceae. 4. Teil: Achnanthaceae. Kritische
923 Ergänzungen zu *Navicula* (Lineolatae) und *Gomphonema*. Gustav Fischer Verlag, Stuttgart, Stuttgart.

924 Kruk, C., M. Devercelli & V. L. Huszar, 2021. Reynolds Functional Groups: a trait-based pathway
925 from patterns to predictions. Hydrobiologia 848: 113–129. https://doi.org/10.1007/s10750-020-04340-
926 9

927 Lair, N. & P. Reyes-Marchant, 1997. The potamoplankton of the Middle Loire and the role of
928 the'moving littoral 'in downstream transfer of algae and rotifers. Hydrobiologia 356: 33–52.

929 Lalot, E., F. Curie, V. Wawrzyniak, F. Baratelli, S. Schomburgk, N. Flipo, H. Piegay & F. Moatar,
930 2015. Quantification of the contribution of the Beauce groundwater aquifer to the discharge of the
931 Loire River using thermal infrared satellite imaging. Hydrology and Earth System Sciences 19: 4479–
932 4492. https://doi.org/10.5194/hess-19-4479-2015

933 Lange-Bertalot, H., 2001. *Navicula sensu stricto*: 10 genera separated from *Navicula sensu lato*
934 *Frustulia*. In Lange-Bertalot, H. (ed) Diatoms of Europe. vol 2. A. R. G. Gantner Verlag K. G.,
935 Königstein, 526 pp.

936 Latapie, A., B. Camenen, S. Rodrigues, A. Paquier, J. P. Bouchard & F. Moatar, 2014. Assessing
937 channel response of a long river influenced by human disturbance. Catena 121: 1–12.
938 https://doi.org/10.1016/j.catena.2014.04.017

939 Legendre, P. & M. J. Anderson, 1999. Distance-based redundancy analysis: testing multispecies
940 responses in multifactorial ecological experiments. Ecological Monographs 69: 1–24.
941 https://doi.org/10.1890/0012-9615(1999)069[0001:DBRATM]2.0.CO;2

942 Legendre, P. & E. Gallagher, 2001. Ecologically meaningful transformations for ordination of species
943 data. Oecologia 129: 271–280. https://doi.org/10.1007/s004420100716

944 Lewis, W. M., Jr, 1978. Dynamics and succession of the phytoplankton in a tropical lake: Lake Lanao,
945 Philippines. The Journal of Ecology 849–880. https://doi.org/10.2307/2259300

946 Litchman, E. & C. A. Klausmeier, 2008. Trait-Based Community Ecology of Phytoplankton. Annual
947 Review of Ecology, Evolution, and Systematics 39: 615–639

34

https://doi.org/10.1146/annurev.ecolsys.39.110707.173

Lohrenz, S. E., C. L. Carroll, A. D. Weidemann & M. Tuel, 2003. Variations in phytoplankton pigments, size structure and community composition related to wind forcing and water mass properties on the North Carolina inner shelf. Continental Shelf Research 23: 1447–1464. https://doi.org/10.1016/S0278-4343(03)00131-6

Loreau, M. & N. Mouquet, 1999. Immigration and the maintenance of local species diversity. The American Naturalist 154: 427–440. https://doi.org/10.1086/303252

Lund, J. W. G. & J. F. Talling, 1957. Botanical limnological methods with special reference to the algae. The Botanical Review 23: 489–583.

Lürling, M., 2021. Grazing resistance in phytoplankton. Hydrobiologia 848: 237–249. https://doi.org/10.1007/s10750-020-04370-3

Minaudo, C., A. Abonyi, M. Leitão, A. M. Lançon, M. Floury, J.-P. Descy & F. Moatar, 2021. Long-term impacts of nutrient control, climate change, and invasive clams on phytoplankton and cyanobacteria biomass in a large temperate river. Science of The Total Environment 756: 144074. https://doi.org/10.1016/j.scitotenv.2020.144074

Minaudo, C., F. Curie, Y. Jullian, N. Gassama & F. Moatar, 2018. QUAL-NET, a high temporal-resolution eutrophication model for large hydrographic networks. Biogeosciences 15: 2251–2269. https://doi.org/10.5194/bg-15-2251-2018

Minaudo, C., M. Meybeck, F. Moatar, N. Gassama & F. Curie, 2015. Eutrophication mitigation in rivers: 30 years of trends in spatial and seasonal patterns of biogeochemistry of the Loire River (1980–2012). Biogeosciences 12: 2549–2563. https://doi.org/10.5194/bg-12-2549-2015

Moatar, F., J.-P. Descy, S. Rodrigues, Y. Souchon, M. Floury, C. Grosbois, C. Minaudo, M. Leitao, K. M. Wantzen & F. Bertrand, 2022. The Loire River basin Rivers of Europe. p. 245–271. In K. Tockner, C. Zarfl, and C. Robinson [eds]. Rivers of Europe. Elsevier. https://doi.org/10.1016/B978-0-08-102612-0.00007-9

Moatar, F. & M. Meybeck, 2005. Compared performances of different algorithms for estimating annual nutrient loads discharged by the eutrophic River Loire. Hydrological Processes 19: 429–444. https://doi.org/10.1002/hyp.5541

Naeem, S., 2008. Species Redundancy and Ecosystem Reliability. Conservation Biology 12: 39–45. https://doi.org/10.1111/j.1523-1739.1998.96379.x

Naselli-Flores, L., T. Zohary & J. Padisák, 2021. Life in suspension and its impact on phytoplankton morphology: an homage to Colin S. Reynolds. Hydrobiologia 848: 7–30. http://dx.doi.org/10.1007/s10750-020-04217-x

35

Nock, C. A., R. J. Vogt & B. E. Beisner, 2016. Functional Traits In John Wiley & Sons, Ltd (ed), eLS. Wiley: 1–8. https://doi.org/10.1002/9780470015902.a0026282

Oksanen, J., 2013. Multivariate Analysis of Ecological Communities in R: vegan tutorial. R package version 1–43.

Oudin, L. C., N. Lair, M. Leitão, P. Reyes-Marchant, J.-F. Mignot, P. Steinbach, T. Vigneron, J.-P. Berton, M. Bacchi, J. E. Roché & J.-P. Descy, 2009. Rivers of Europe (Eds Tockner K. & C.T. Robinson). British Library, London.

Padisák, J., L. O. Crossetti & L. Naselli-Flores, 2009. Use and misuse in the application of the phytoplankton functional classification: a critical review with updates. Hydrobiologia 621: 1–19. https://doi.org/10.1007/s10750-008-9645-0

Padisák, J., E. Soróczki-Pintér & Z. Rezner, 2003. Sinking properties of some phytoplankton shapes and the relation of form resistance to morphological diversity of plankton—an experimental study. Hydrobiologia 500: 243-257. https://doi.org/10.1007/978-94-007-1084-9

Pančić, M. & T. Kiørboe, 2018. Phytoplankton defence mechanisms: traits and trade-offs. Biological Reviews 93: 1269–1303. https://doi.org/10.1111/brv.12395

Pannard, A., M. Bormans & Y. Lagadeuc, 2008a. Phytoplankton species turnover controlled by physical forcing at different time scales. Canadian Journal of Fisheries and Aquatic Sciences 65: 47–60. https://doi.org/10.1139/F07-149

Pannard, A., P. Claquin, C. Klein, B. Le Roy & B. Véron, 2008b. Short-term variability of the phytoplankton community in coastal ecosystem in response to physical and chemical conditions' changes. Estuarine, Coastal and Shelf Science 80: 212–224. https://doi.org/10.1016/j.ecss.2008.08.008

Pathak, D., M. Hutchins, L. Brown, M. Loewenthal, P. Scarlett, L. Armstrong, D. Nicholls, M. Bowes & F. Edwards, 2021. Hourly Prediction of Phytoplankton Biomass and Its Environmental Controls in Lowland Rivers. Water Resources Research 57: 1-20. https://doi.org/10.1029/2020WR028773

Peterson, B., B. Fry, M. Hullar, S. Saupe & R. Wright, 1994. The distribution and stable carbon isotopic composition of dissolved organic carbon in estuaries. Estuaries 17: 111–121.

Peterson, C. G. & R. J. Stevenson, 1989. Seasonality in river phytoplankton: multivariate analyses of data from the Ohio River and six Kentucky tributaries. Hydrobiologia 182: 99–114.

Picard, V. & N. Lair, 2005. Spatio-temporal investigations on the planktonic organisms of the Middle Loire (France), during the low water period: biodiversity and community dynamics. Hydrobiologia 551: 69–86. https://doi.org/10.1007/s10750-005-4451-4

Pickett, S. & P.S.White, 1985. The ecology of natural disturbance and patch dynamics, Pickett, STA and PS White (Ed.). the Ecology of Natural Disturbance and Patch Dynamics. Orlando, Fla, USA.

36

Popovský, J. & L. A. Pfiester, 1990. Dinophyceae (Dinoflagellida). Gustav Fischer Verlag, Stuttgart, 272 pp.

Ptacnik, R., T. Andersen & T. Tamminen, 2010. Performance of the Redfield Ratio and a Family of Nutrient Limitation Indicators as Thresholds for Phytoplankton N vs. P Limitation. Ecosystems 13: 1201–1214. https://doi.org/10.1007/s10021-010-9380-z

Reddy, K. R., O. A. Diaz, L. J. Scinto & M. Agami, 1995. Phosphorus dynamics in selected wetlands and streams of the Lake Okeechobee Basin. Ecological Engineering 5(2-3): 183-207. https://doi.org/10.1016/0925-8574(95)00024-0

Reynolds, C. S., 1984. Phytoplankton periodicity: the interactions of form, function and environmental variability. Freshwater Biology 14: 111–142.

Reynolds, C. S., 2006. The ecology of phytoplankton. Cambridge University Press.

Reynolds, C. S. & J.-P. Descy, 1996. The production, biomass and structure of phytoplankton in large rivers. Large Rivers. Archiv für Hydrobiologie Supplement 10 (1–4): 161–187. https://doi.org/10.1127/lr/10/1996/161

Reynolds, C. S., J.-P. Descy & J. Padisák, 1994. Are phytoplankton dynamics in rivers so different from those in shallow lakes ? Hydrobiologia 289: 1–7.

Rojo, C., M. A. Cobelas & M. Arauzo, 1994. An elementary, structural analysis of river phytoplankton. Hydrobiologia 289: 43–55.

Rott, E., 1981. Some results from phytoplankton counting intercalibrations. Schweizerische Zeitschrift für Hydrologie 43: 34–62. https://doi.org/10.1007/BF02502471

Sabater, S., J. Artigas, C. Durán, M. Pardos, A. M. Romaní, E. Tornés & I. Ylla, 2008. Longitudinal development of chlorophyll and phytoplankton assemblages in a regulated large river (the Ebro River). Science of The Total Environment 404: 196–206. https://doi.org/10.1016/j.scitotenv.2008.06.013

Salmaso, N., L. Naselli-Flores & J. Padisák, 2015. Functional classifications and their application in phytoplankton ecology. Freshwater Biology 60: 603–619. https://doi.org/10.1111/fwb.12520

Seyedhashemi, H., J.-P. Vidal, J. S. Diamond, D. Thiéry, C. Monteil, F. Hendrickx, A. Maire & F. Moatar, 2022. Regional, multi-decadal analysis on the Loire River basin reveals that stream temperature increases faster than air temperature. Hydrology and Earth System Sciences 26: 2583–2603. https://doi.org/10.5194/hess-26-2583-2022

Smith, T. E., R. J. Stevenson, N. F. Caraco & J. J. Cole, 1998. Changes in phytoplankton community structure during the zebra mussel (*Dreissena polymorpha*) invasion of the Hudson River (New York). Journal of Plankton Research 20: 1567–1579.

Starmach, K., 1985. Chrysophyceae und Haptophyceae. Gustav Fischer Verlag, Stuttgart, 515 pp.

37

1047 Strickland JDH & T.R. Parsons, 1972. A Practical Handbook of Seawater Analysis (2nd ed.). Fisheries
1048 Research Board of Canada, Ottawa, Bulletin 167. https://doi.org/10.1086/406210

1049 Utermöhl, H., 1958. Zur Vervollkommnung der quantitativen Phytoplankton-Methodik. Mitteilungen
1050 Internationale Ver- einigung Fuer Theoretische Und Angewandte Limnologie 9: 1–38.

1051 Vannote, R. L., G. W. Minshall, K. W. Cummins, J. R. Sedell & C. E. Cushing, 1980. The river
1052 continuum concept. Canadian Journal of Fisheries and Aquatic Sciences 37: 130–137.

1053 Várbíró, G., J. Padisák, Z. Nagy-László, A. Abonyi, I. Stanković, M. Gligora Udovič, V. B-Béres &
1054 G. Borics, 2018. How length of light exposure shapes the development of riverine algal biomass in
1055 temperate rivers? Hydrobiologia 809: 53–63. https://doi.org/10.1007/s10750-017-3447-1

1056 Violle, C., M.-L. Navas, D. Vile, E. Kazakou, C. Fortunel, I. Hummel & E. Garnier, 2007. Let the
1057 concept of trait be functional! Oikos 116: 882–892. https://doi.org/10.1111/j.0030-1299.2007.15559.x

1058 Wade, A. J., E. J. Palmer-Felgate, S. J. Halliday, R. A. Skeffington, M. Loewenthal, H. P. Jarvie, M. J.
1059 Bowes, G. M. Greenway, S. J. Haswell, I. M. Bell, E. Joly, A. Fallatah, C. Neal, R. J. Williams, E.
1060 Gozzard & J. R. Newman, 2012. Hydrochemical processes in lowland rivers: insights from in situ,
1061 high-resolution monitoring. Hydrology and Earth System Sciences 16: 4323–4342.
1062 https://doi.org/10.5194/hess-16-4323-2012

1063 Wang, C., Li, X., Lai, Z., Li, Y., Dauta, A. & S. Lek, 2014. Patterning and predicting phytoplankton
1064 assemblages in a large subtropical river. Fundamental and Applied Limnology 185: 263-279.
1065 https://doi.org/10.1127/fal/2014/0684

1066 Wang, C., Baehr, C., Lai, Z., Gao, Y., Lek, S. & X. Li, 2015. Exploring temporal trend of
1067 morphological variability of a dominant diatom in response to environmental factors in a large
1068 subtropical river. Ecological Informatics 29: 96-106. https://doi.org/10.1016/j.ecoinf.2014.11.002

1069 Wawrzyniak, V., P. Allemand, S. Bailly, J. Lejot & H. Piégay, 2017. Coupling LiDAR and thermal
1070 imagery to model the effects of riparian vegetation shade and groundwater inputs on summer river
1071 temperature. Science of The Total Environment 592: 616–626.
1072 https://doi.org/10.1016/j.scitotenv.2017.03.019

1073 Wehr, J. D. & J.-P. Descy, 1998. Use of phytoplankton in large river management. Journal of
1074 Phycology 34: 741–749.

1075 Wehr, J. D., R. G. Sheath & J. P. Kociolek, 2015. Freshwater algae of North America: ecology and
1076 classification. Elsevier.

1077 Wei, T. & V. Simko, 2017. R package "corrplot": Visualization of a Correlation Matrix (Version
1078 0.84). Available from https://github.com/taiyun/corrplot.

1079 Winder, M., J. E. Reuter & S. G. Schladow, 2008. Temporal organization of phytoplankton

38

communities linked to physical forcing. Oecologia 156: 179–192. https://doi.org/10.1007/s00442-008-0964-7

Wu, N., B. Schmalz & N. Fohrer, 2011. Distribution of phytoplankton in a German lowland river in relation to environmental factors. Journal of Plankton Research 33: 807-820. https://doi.org/10.1093/plankt/fbq139

Wu, N., Faber, C., Sun, X., Qu, Y., Wang, C., Ivetic, S., Riis, T., Ulrich, U. & N. Fohrer, 2016. Importance of sampling frequency when collecting diatoms. Scientific reports 6(1): 36950. https://doi.org/10.1038/srep36950

39

1088 **FIGURE CAPTIONS**

1089 **Figure 1**. Identification of hydrological events and associated periods. An increase in the slope dF/dt
1090 between two consecutive days highlights the beginning of a disturbance and is noticed t*. The
1091 'Before' period corresponds to the seven days preceding t* and begins on day t_1 (t_1 = t* - 7days). The
1092 'After' period corresponds to the disturbed period, extending from day t* to the return to stable
1093 conditions on day t_2.

1094 **Figure 2**. Time series in summer 2013 (a) of the river flow Q and the ratio particulate organic carbon :
1095 chlorophyll-a (POC:Chl-a), with the same y-axis scale, (b) of concentration in suspended matter, (c) of
1096 dissolved inorganic phosphorus (DIP) concentration, (d) of dissolved organic carbon concentration, (e)
1097 of chlorophyll-a and pheopigments concentrations, and (f) of the inverse Simpson's index. Vertical red
1098 dotted line shows the main disturbances with their numbering. Periods identified are shown at the top
1099 of the figure.

1100 **Figure 3**. CCA performed on phytoplankton assemblages from 2013 explained by environmental
1101 parameters (p=0.001). (a) Plot of the taxa. Only taxa contributing to at least 1% to canonical axis are
1102 shown. (b) Plot of the environmental parameters (Q: water discharge; SM: suspended matter; Nitrates:
1103 nitrates concentration; DSi: DSi concentration; DIP: dissolved inorganic phosphorus concentration;
1104 Temperature; DOC: dissolved organic carbon concentration; pH; DO: Dissolved Oxygen). (c) Plot of
1105 the sampling dates, grouped afterwards according to the period (Bef1: before 1; Bef2: before 2; Aft1:
1106 After 1; Aft2: After 2; Aft3: After 3; Aft4: After 4; Stable 1; Stable 2) See Fig. 2 for periods' details.
1107 Scale of x and y axes is given by d value at the top right for each plot.

1108 **Figure 4**. Time series of phytoplankton taxa biovolumes in mg C L^{-1} during summer 2013, with (a)
1109 *Nitzschia acicularis*, (b) *Skeletonema potamos,* (c) *Chlamydomonas sp*., (d) *Golenkinia radiata*, (e)
1110 *Actinastrum hantzschii*, (f) *Scenedesmus* spp. 3 and (g) *Diatoma vulgaris*. Periods identified are shown
1111 at the top of the figure.

1112 **Figure 5**. Time series in summer 2014 (a) of the river flow Q and the ratio particulate organic carbon :
1113 chlorophyll-a (POC:Chl-a), with the same y-axis scale, (b) of concentration in suspended matter, (c) of
1114 dissolved inorganic phosphorus (DIP) concentration, (d) of dissolved organic carbon concentration, (e)
1115 of chlorophyll-a and pheopigments concentrations, and (f) of the inverse Simpson's index. Vertical red

40

dotted line shows the main disturbances with their numbering. Periods identified are shown at the top of the figure.

Figure 6. CCA performed on phytoplankton assemblages from 2014 explained by environmental parameters (p=0.029). (a) Plot of the taxa. Only taxa contributing to at least 1% to canonical axis are shown. (b) Plot of the environmental parameters (Q: water discharge; SM: suspended matter; Nitrates: nitrates concentration; DSi: DSi concentration; DIP: dissolved inorganic phosphorus concentration; Temperature; DOC: dissolved organic carbon concentration; DO: Dissolved Oxygen). (c) Plot of the sampling dates, grouped afterwards according to the period (Bef1: before 1; Bef2: before 2; Aft1: After 1; Aft2: After 2; Aft3: After 3; Aft4: After 4; Stable) See Fig. 2 for periods' detail. Scale of x and y axes is given by d value at the top right for each plot.

Figure 7. Time series of phytoplankton taxa biovolumes in mg C L^{-1} during summer 2014, with (a) *Monoraphidium* spp., (b) *Kirchneriella* spp., (c) *Tetraedron* spp., (d) *Skeletonema potamos*, (e) *Merismopedia* spp., (f) *Acutodesmus* spp. and (g) *Nitzschia acicularis*. Periods identified are shown at the top of the figure.

Figure 8. Illustration of species representative of the three periods, showing their morphometry and traits: stable assemblages with A2 and B1; disturbed assemblage with A1 and B2; repeatedly disturbed assemblage with A3 and B3. RFG are indicated near each draw. Taxa framed with a dotted blue line are observed at least over two periods. Taxa framed in a red line are observed in the same period both years. 1. *Nitzschia acicularis* (Kützing) W.M.Smith and *N. dissipata* (Kützing) Grunow; 2. *Dictyosphaerium pulchellum* Wood; 3. *Tetrastrum triangulare* (Chodat) Komárek ; 4. *Actinastrum hantzschii* Lagerheim; 5. *Golenkinia radiata* Chodat; 6. *Monoraphidium contortum* (Thuret) Komárková-Legnerová; 7. *Lobomonas ampla* Pascher; 8. *Franceia ovalis* (France) Lemmermann; 9. *Plagioselmis nannoplanctica* (H. Skuja) G. Novarino, I.A.N. Lucas & S. Morrall; 10. *Didymocystis planctonica* Korshikov; 11. *Oocystis lacustris* Chodat; 12. *Micractinium pusillum* Fresenius; 13. *Treubaria planctonica* (G.M.Smith) Korshikov; 14. *Scenedesmus* spp. Meyen (with for example *Scenedesmus* group *Armati sensu* Komárek & Fott), *Acutodesmus* spp. (Hegewald) Tsarenko and *Desmodesmus* spp. (R.Chodat) S.S.An, T.Friedl & E.Hegewald ; 15. *Kirchneriella lunaris* (Kirchner) Möbius; 16. *Coelastrum microporum* Nägeli; 17. *Tetraedron minimum* (A.Braun)

41

Hansgirg; 18. *Chlamydomonas* sp. Ehrenberg; 19. *Skeletonema potamos* (Weber) Hasle; 20. *Merismopedia tenuissima* Lemmermann; 21. *Diatoma vulgaris* Bory.

Figure 9. (a) Plot of the two axes of the discriminant Analysis (DA) performed on phytoplankton RFG. The discriminant factor is one of the three assemblages (stable, repeated, repeatedly disturbed) and each sample is attached to the gravity center of the group it belongs to. (b) Correlation circle plot showing the phytoplankton RFG. Scale of x and y axes is given by d value at the top right for each plot.

Figure 10. Pearson's correlation matrix between log10-transformed RFG and taxa and environmental parameters: Q river discharge, T° daily mean water temperature, DO daily mean dissolved oxygen, daily mean pH, Cd daily mean conductivity, SM suspended matter, Ry solar radiations, Nitr. Nitrates, DIP, DSi and COD concentrations. Significativity of the Pearson's correlation is shown: *means $p<0.05$, ** $p< 0.01$ and *** $p<0.001$. Colored ellipses indicate the positive (blue) or negative (red) correlations.

Figure S1. Time series of environmental and biological parameters at the station Cinq-Mars-La-Pile. Q: water discharge; SM: suspended matter; Nitrates: nitrates concentration; TP: total phosphorus concentration; DSi: silicate concentration; POC: particulate organic carbon; Temp.: temperature; radiation: solar radiation; Chl-a: total pigment concentration; DIP: dissolved inorganic phosphorus concentration; DOC: dissolved organic carbon concentration; Phy biom: phytoplankton biomass calculated from cell counts and grouped by class; Tot biom: total phytoplankton biomass calculated from cell counts; Turnover: turnover rate per day.

Figure S2. Variance partitioning of taxa biomass depending on time with julian day (X1), water temperature (X2) and dissolved inorganic phosphorus (X3), performed with the function *varpart* of the package vegan. The analysis was performed on all data, on summer 2013 and on summer 2014.

42

Figure 1.

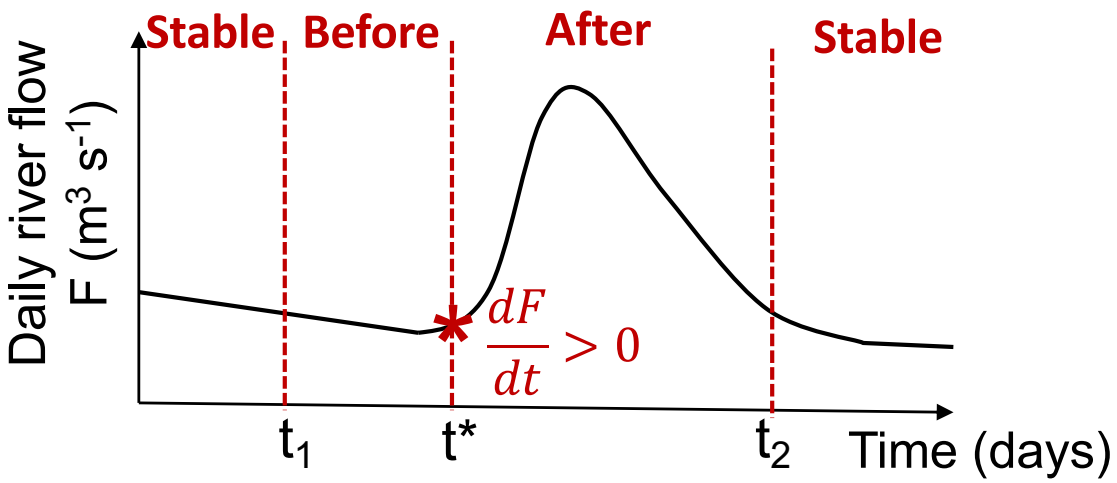
Stable
Before
After
Stable
Daily river flow
F (m3 s-1)
dF/dt > 0
t1
t*
t2
Time (days)

Figure 2.

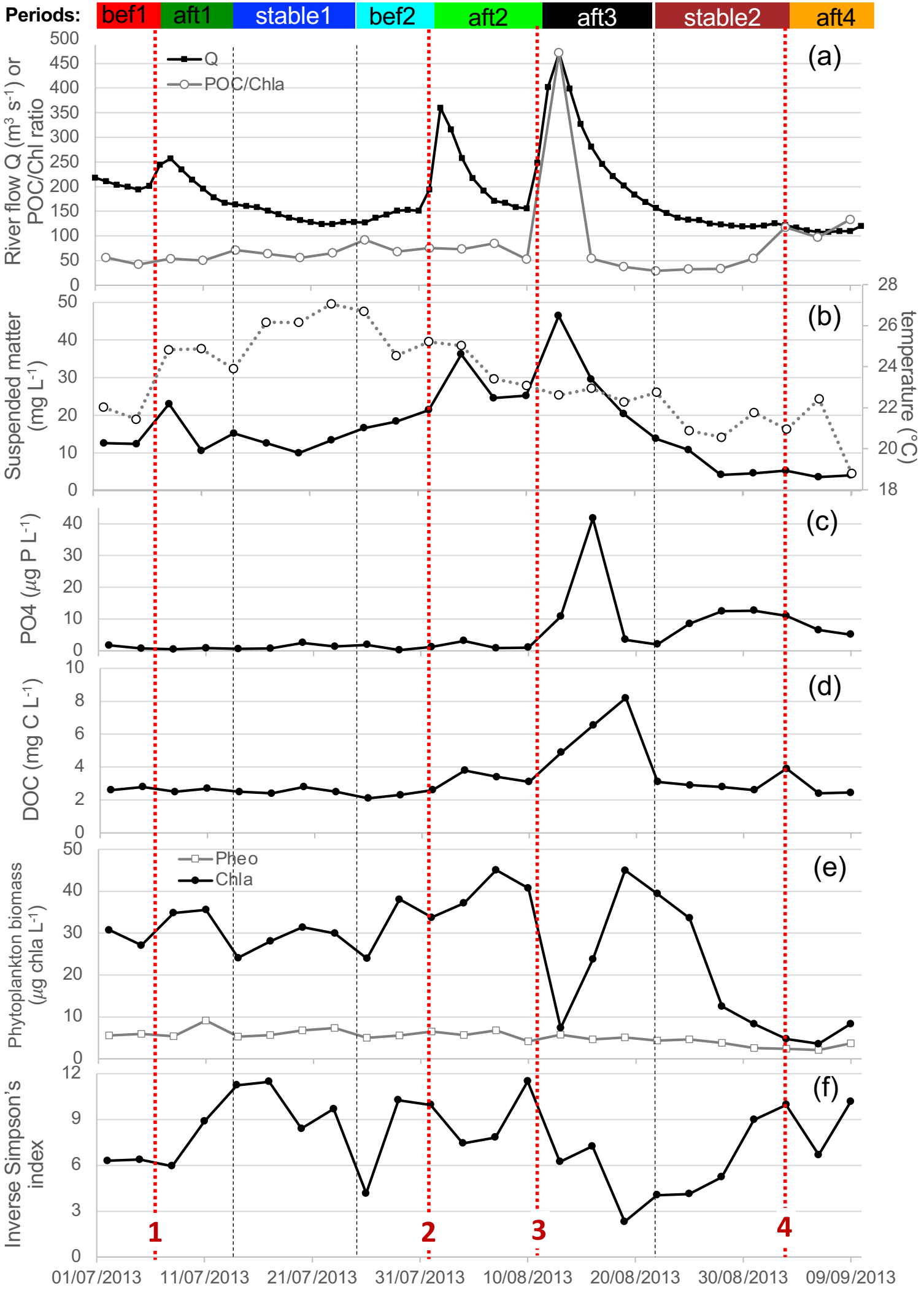
Periods:
bef1
aft1
stable1
bef2
aft2
aft3
stable2
aft4
(a)
River flow Q (m³ s⁻¹) or POC/Chl ratio
Q
POC/Chla
(b)
Suspended matter (mg L⁻¹)
temperature (°C)
(c)
PO4 (µg P L⁻¹)
(d)
DOC (mg C L⁻¹)
(e)
Phytoplankton biomass (µg chla L⁻¹)
Pheo
Chla
(f)
Inverse Simpson's index
1
2
3
4
01/07/2013
11/07/2013
21/07/2013
31/07/2013
10/08/2013
20/08/2013
30/08/2013
09/09/2013

Figure 3.

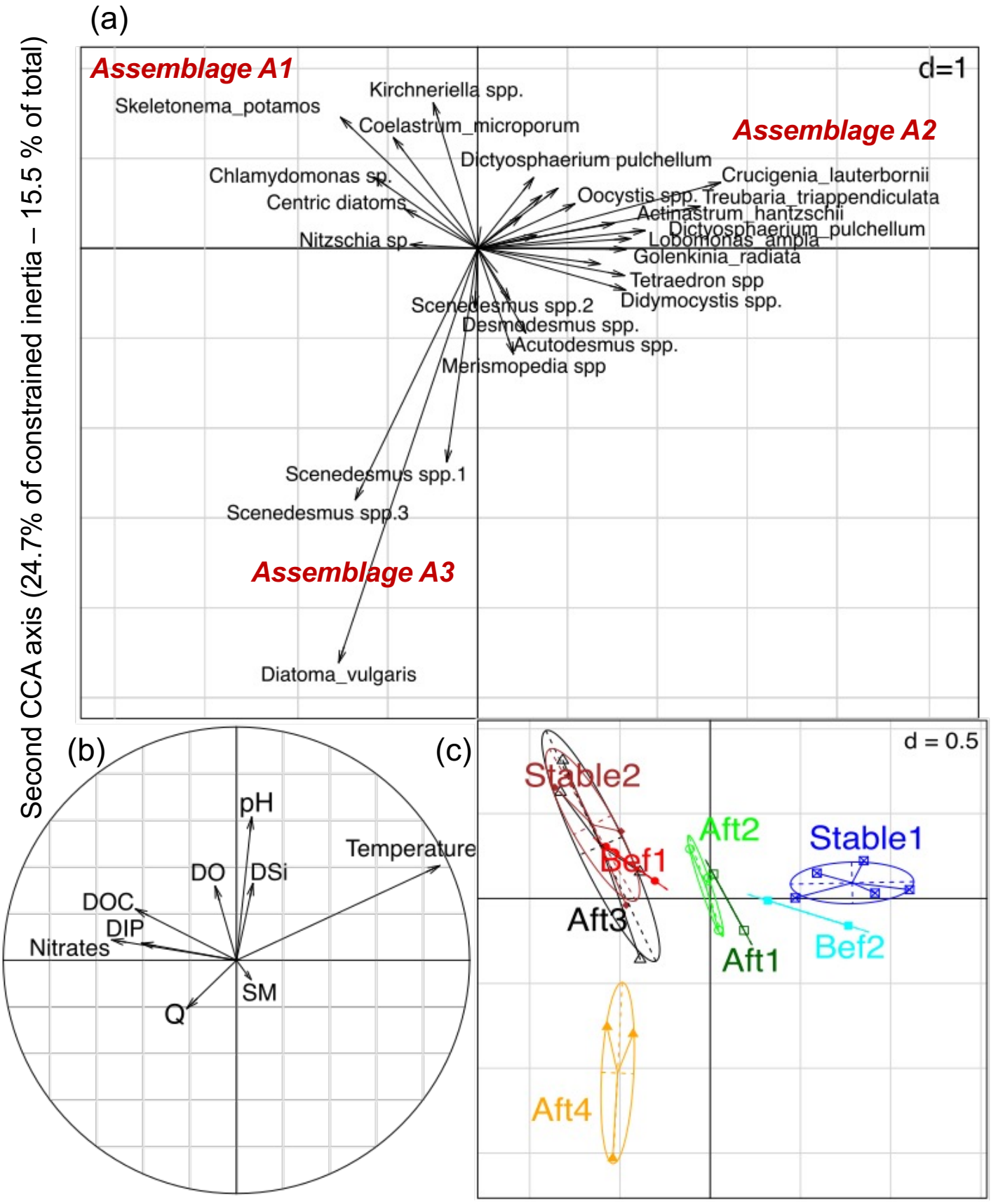

First CCA axis (38.8 % of constrained inertia – 24.3% of total variance)

Figure 4.

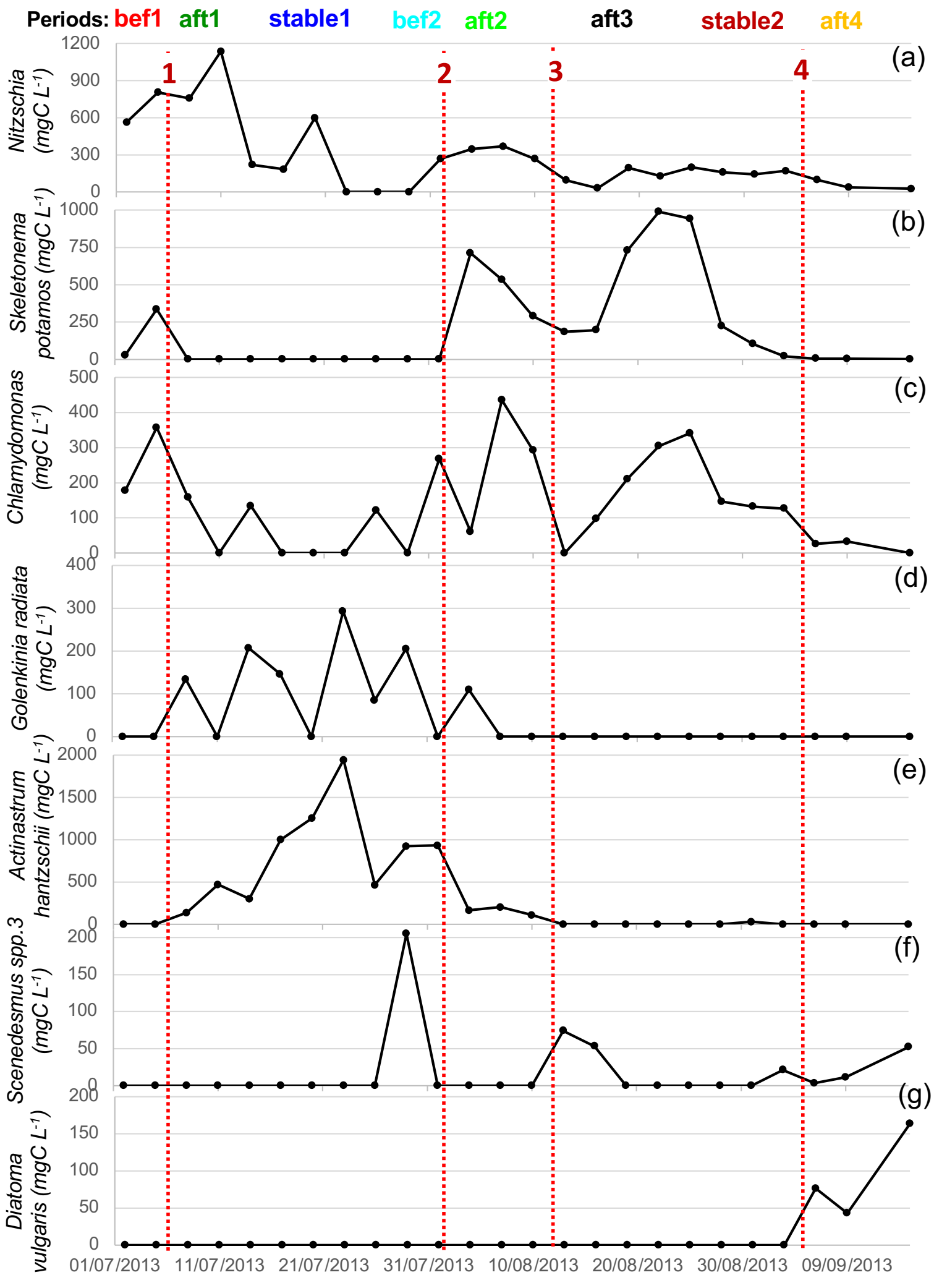
Periods: bef1 aft1 stable1 bef2 aft2 aft3 stable2 aft4
1
2
3
4
(a)
Nitzschia (mgC L-1)
1200
900
600
300
0
(b)
Skeletonema potamos (mgC L-1)
1000
750
500
250
0
(c)
Chlamydomonas (mgC L-1)
500
400
300
200
100
0
(d)
Golenkinia radiata (mgC L-1)
400
300
200
100
0
(e)
Actinastrum hantzschii (mgC L-1)
2000
1500
1000
500
0
(f)
Scenedesmus spp.3 (mgC L-1)
200
150
100
50
0
(g)
Diatoma vulgaris (mgC L-1)
200
150
100
50
0
01/07/2013
11/07/2013
21/07/2013
31/07/2013
10/08/2013
20/08/2013
30/08/2013
09/09/2013

Figure 5.

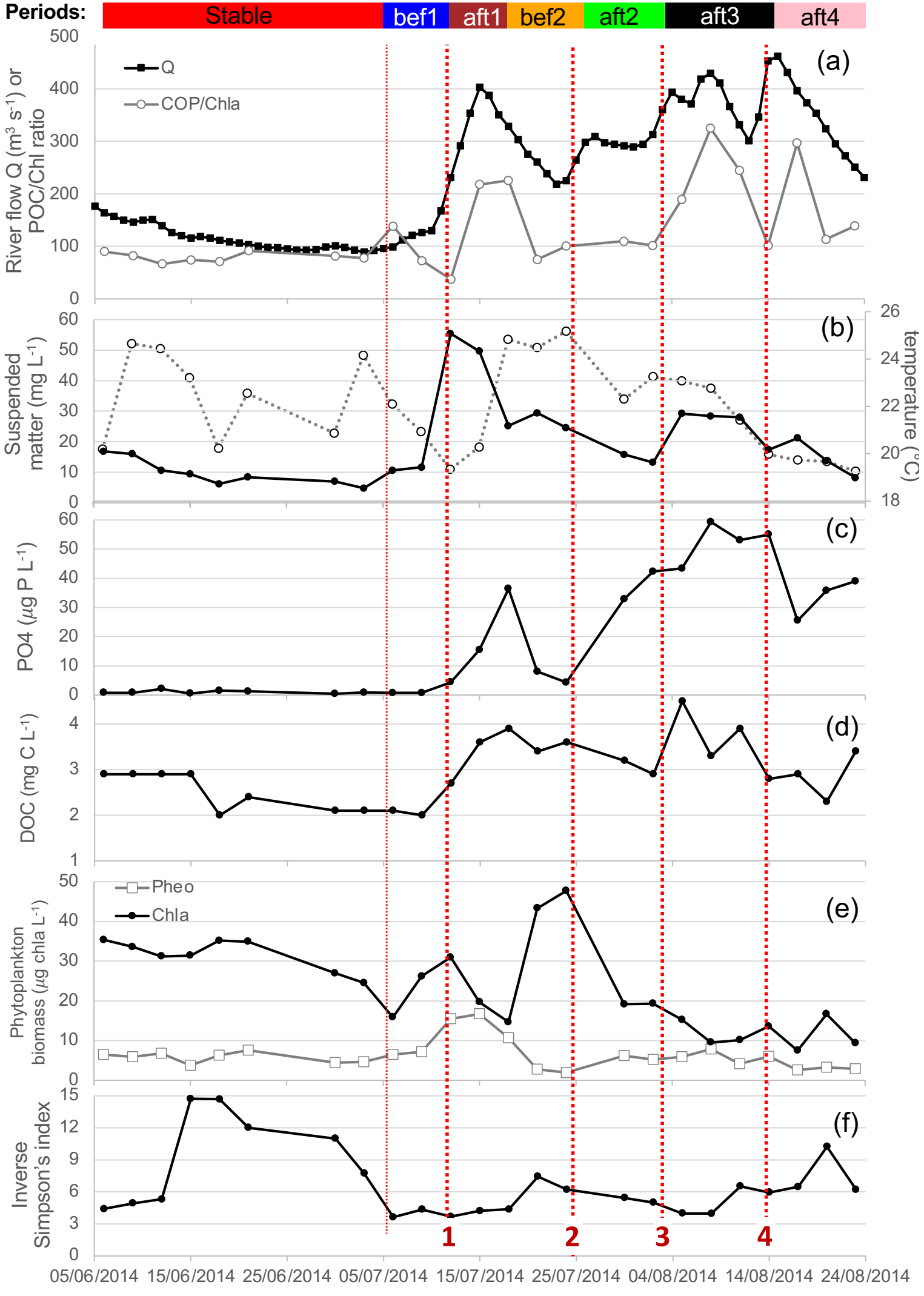
Periods:
Stable
bef1
aft1
bef2
aft2
aft3
aft4
(a)
River flow Q (m³ s⁻¹) or POC/Chl ratio
Q
COP/Chla
(b)
Suspended matter (mg L⁻¹)
temperature (°C)
(c)
PO4 (µg P L⁻¹)
(d)
DOC (mg C L⁻¹)
(e)
Phytoplankton biomass (µg chla L⁻¹)
Pheo
Chla
(f)
Inverse Simpson's index
1
2
3
4
05/06/2014
15/06/2014
25/06/2014
05/07/2014
15/07/2014
25/07/2014
04/08/2014
14/08/2014
24/08/2014

Figure 6.

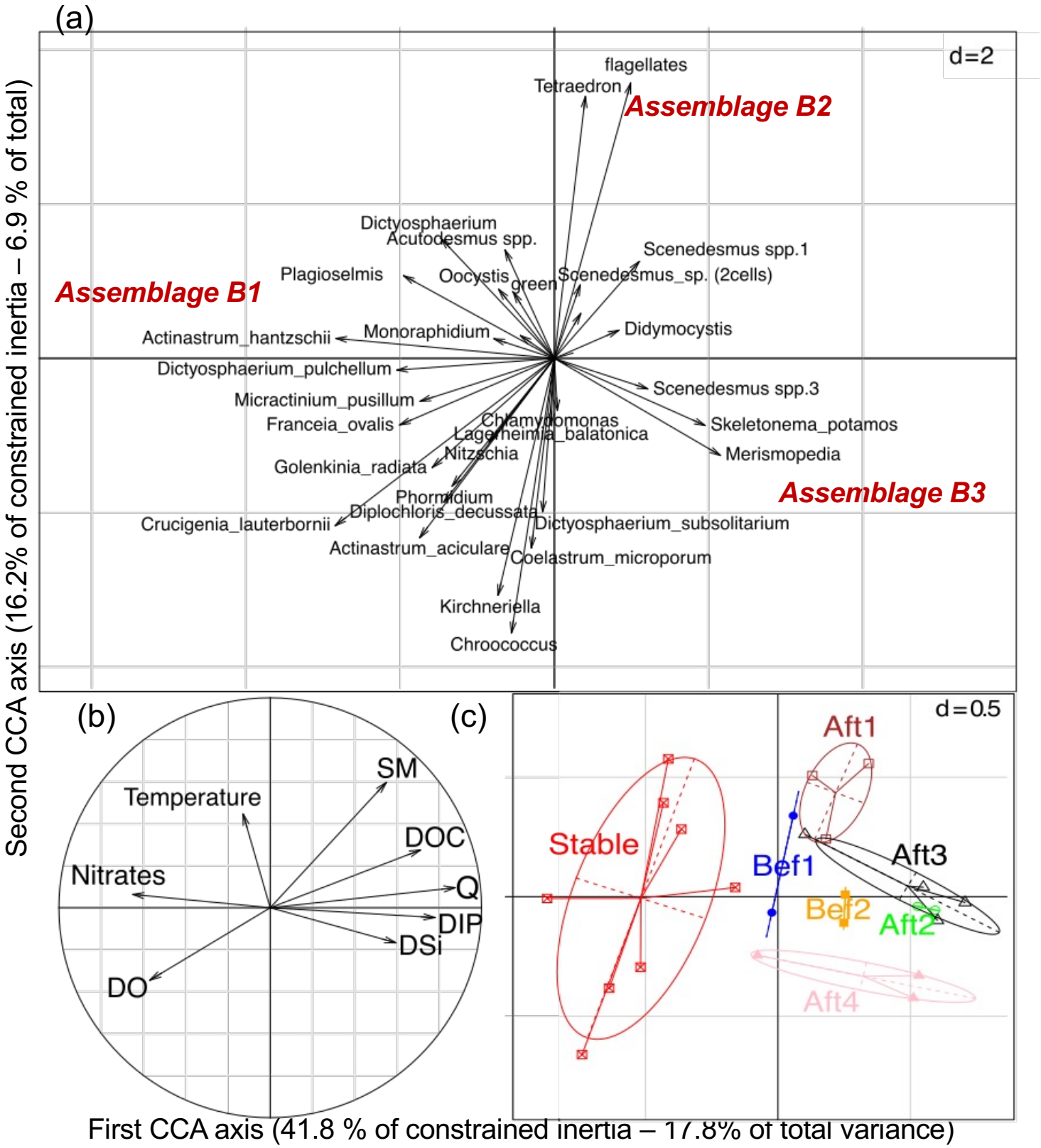
(a)
d=2
flagellates
Tetraedron
Assemblage B2
Dictyosphaerium
Acutodesmus spp.
Scenedesmus spp.1
Plagioselmis
Oocystis
green
Scenedesmus_sp. (2cells)
Assemblage B1
Actinastrum_hantzschii
Monoraphidium
Didymocystis
Dictyosphaerium_pulchellum
Scenedesmus spp.3
Micractinium_pusillum
Franceia_ovalis
Chlamydomonas
Lagerheimia_balatonica
Skeletonema_potamos
Nitzschia
Merismopedia
Golenkinia_radiata
Assemblage B3
Phormidium
Diplochloris_decussata
Crucigenia_lauterbornii
Dictyosphaerium_subsolitarium
Actinastrum_aciculare
Coelastrum_microporum
Kirchneriella
Chroococcus
(b)
SM
Temperature
DOC
Nitrates
Q
DIP
DSi
DO
(c)
d=0.5
Aft1
Stable
Bef1
Aft3
Bef2
Aft2
Aft4
Second CCA axis (16.2% of constrained inertia – 6.9 % of total)
First CCA axis (41.8 % of constrained inertia – 17.8% of total variance)

Figure 7.

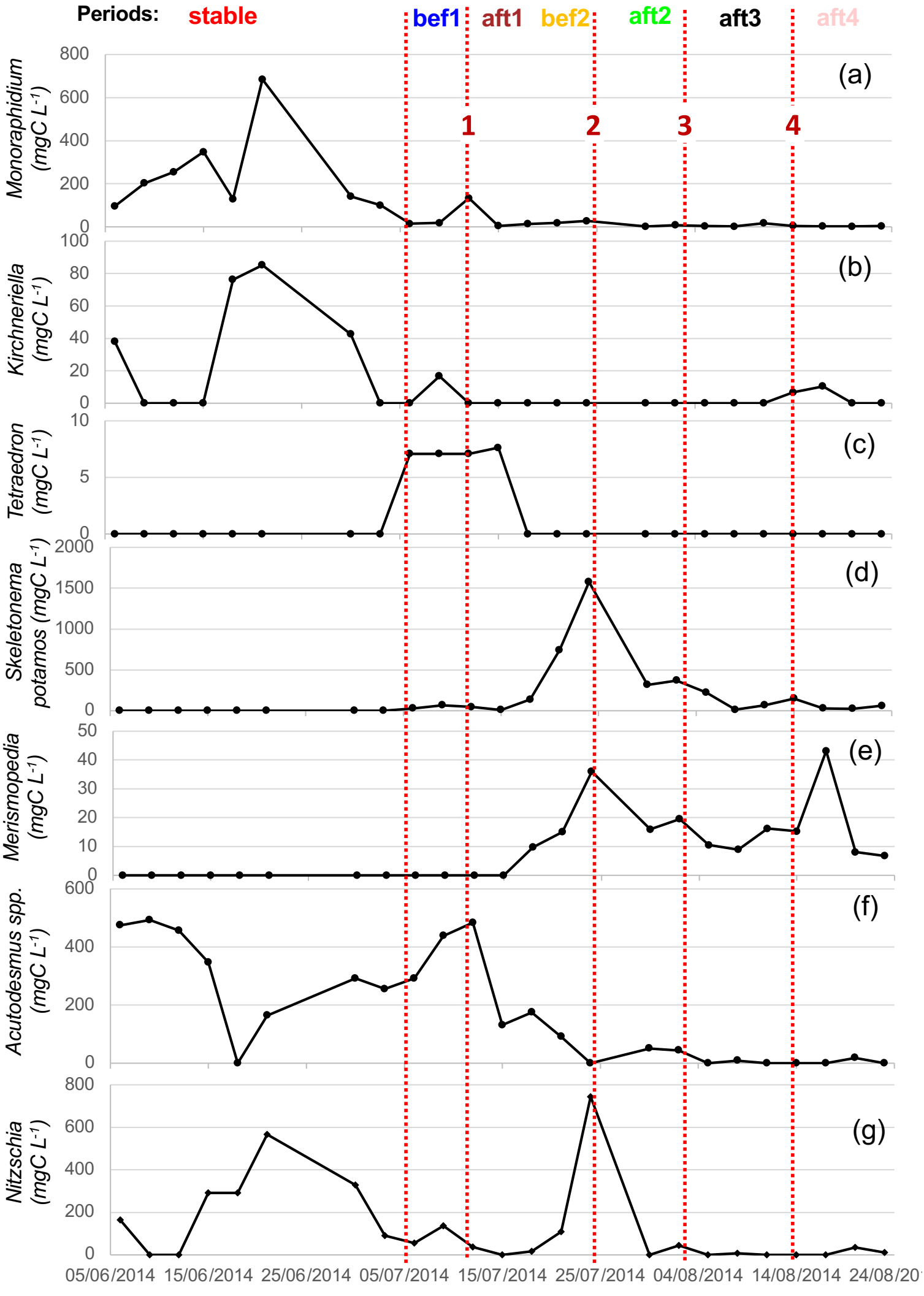
Periods:
stable
bef1
aft1
bef2
aft2
aft3
aft4
1
2
3
4
(a)
Monoraphidium (mgC L-1)
800
600
400
200
0
(b)
Kirchneriella (mgC L-1)
100
80
60
40
20
0
(c)
Tetraedron (mgC L-1)
10
5
0
(d)
Skeletonema potamos (mgC L-1)
2000
1500
1000
500
0
(e)
Merismopedia (mgC L-1)
50
40
30
20
10
0
(f)
Acutodesmus spp. (mgC L-1)
600
400
200
0
(g)
Nitzschia (mgC L-1)
800
600
400
200
0
05/06/2014
15/06/2014
25/06/2014
05/07/2014
15/07/2014
25/07/2014
04/08/2014
14/08/2014
24/08/20

Figure 8.

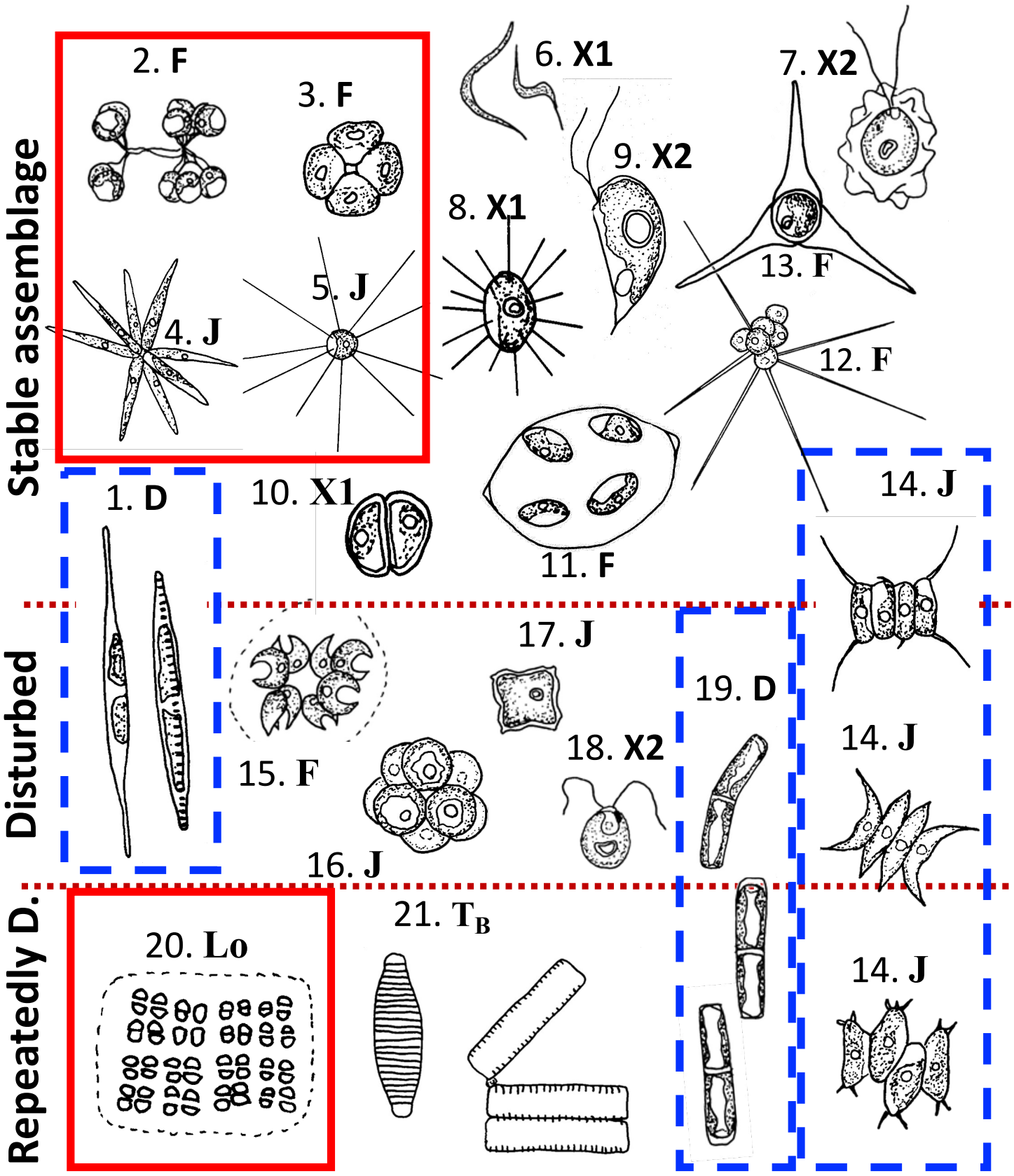

@drawings from Maria Leitao

Figure 9.

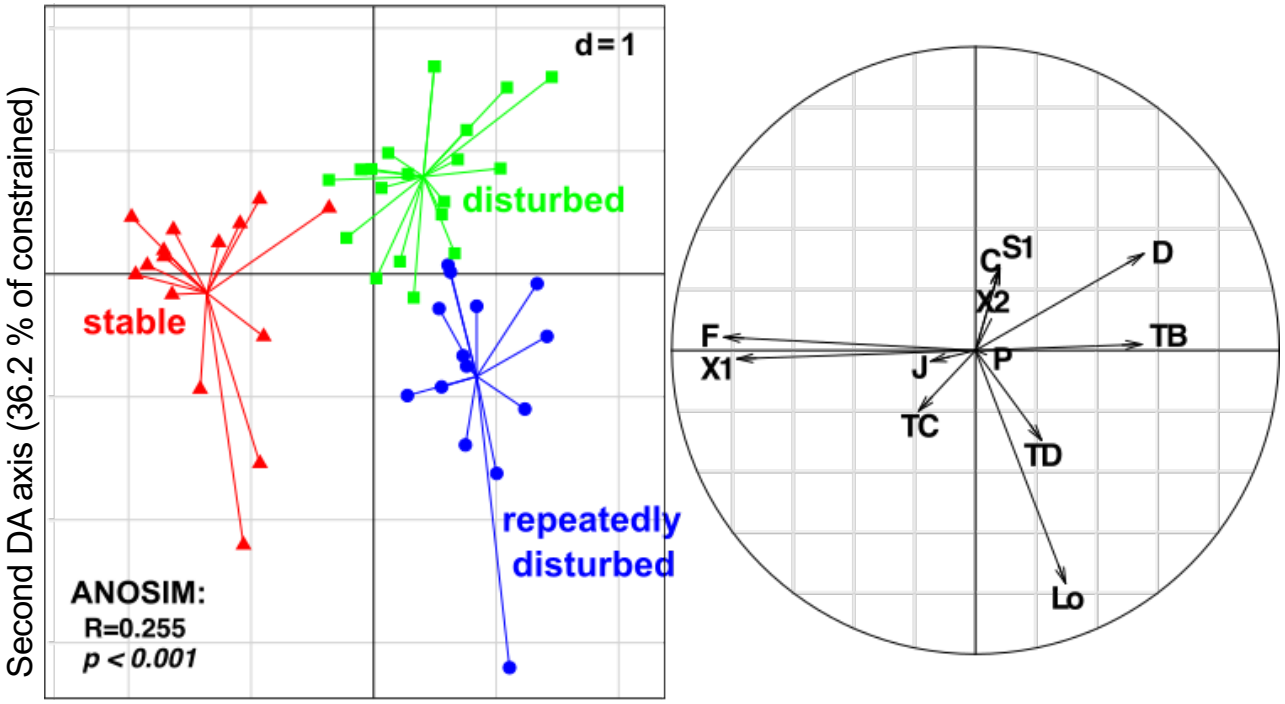
d=1
disturbed
stable
repeatedly
disturbed
ANOSIM:
R=0.255
p < 0.001
Second DA axis (36.2 % of constrained)
First DA axis (63.8 % of constrained variance)
S1
D
X2
F
TB
X1
J
P
TC
TD
Lo

Figure 10.

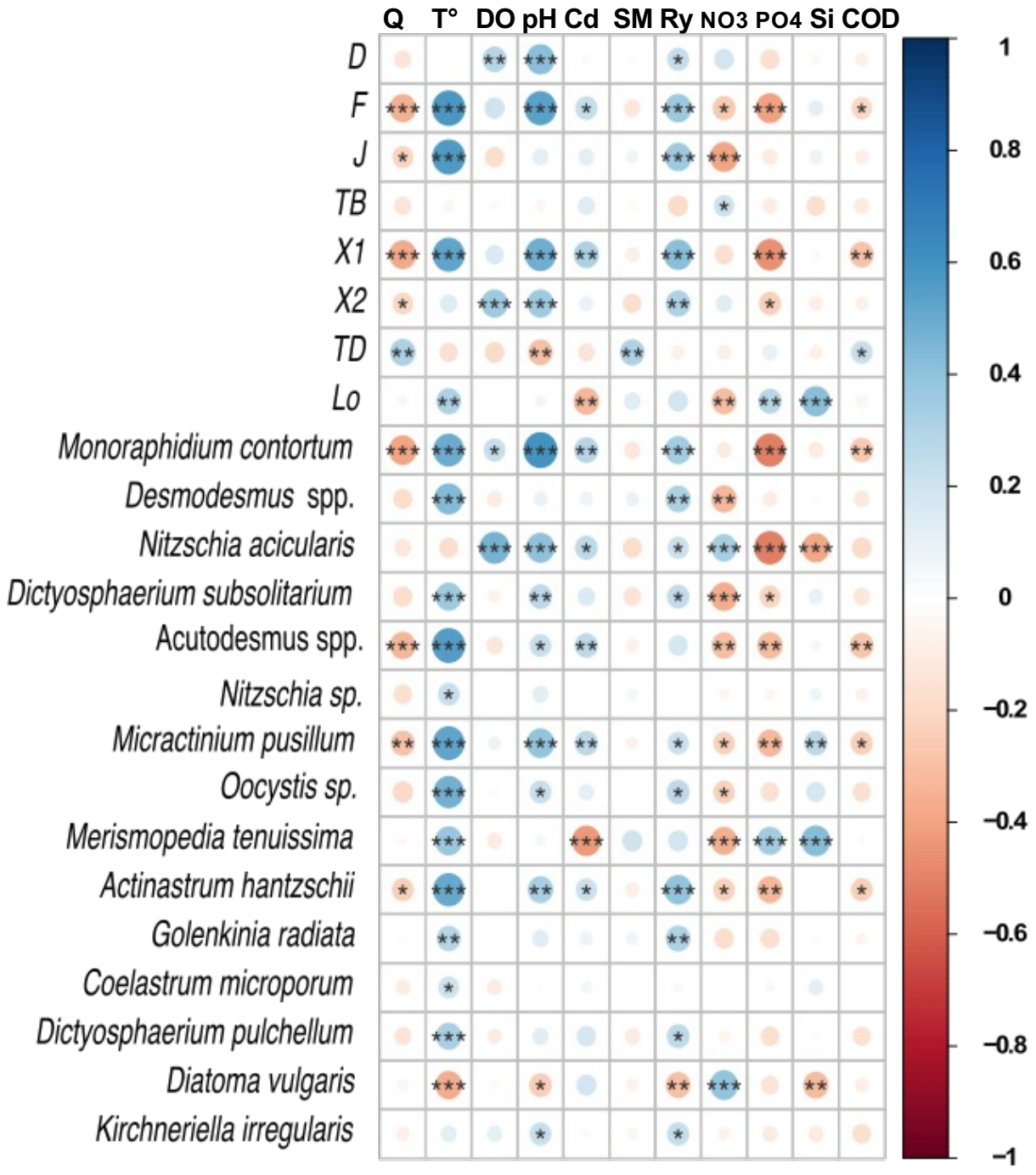
Q
T°
DO
pH
Cd
SM
Ry
NO3
PO4
Si
COD
D
F
J
TB
X1
X2
TD
Lo
Monoraphidium contortum
Desmodesmus spp.
Nitzschia acicularis
Dictyosphaerium subsolitarium
Acutodesmus spp.
Nitzschia sp.
Micractinium pusillum
Oocystis sp.
Merismopedia tenuissima
Actinastrum hantzschii
Golenkinia radiata
Coelastrum microporum
Dictyosphaerium pulchellum
Diatoma vulgaris
Kirchneriella irregularis
1
0.8
0.6
0.4
0.2
0
−0.2
−0.4
−0.6
−0.8
−1

Figure S1.

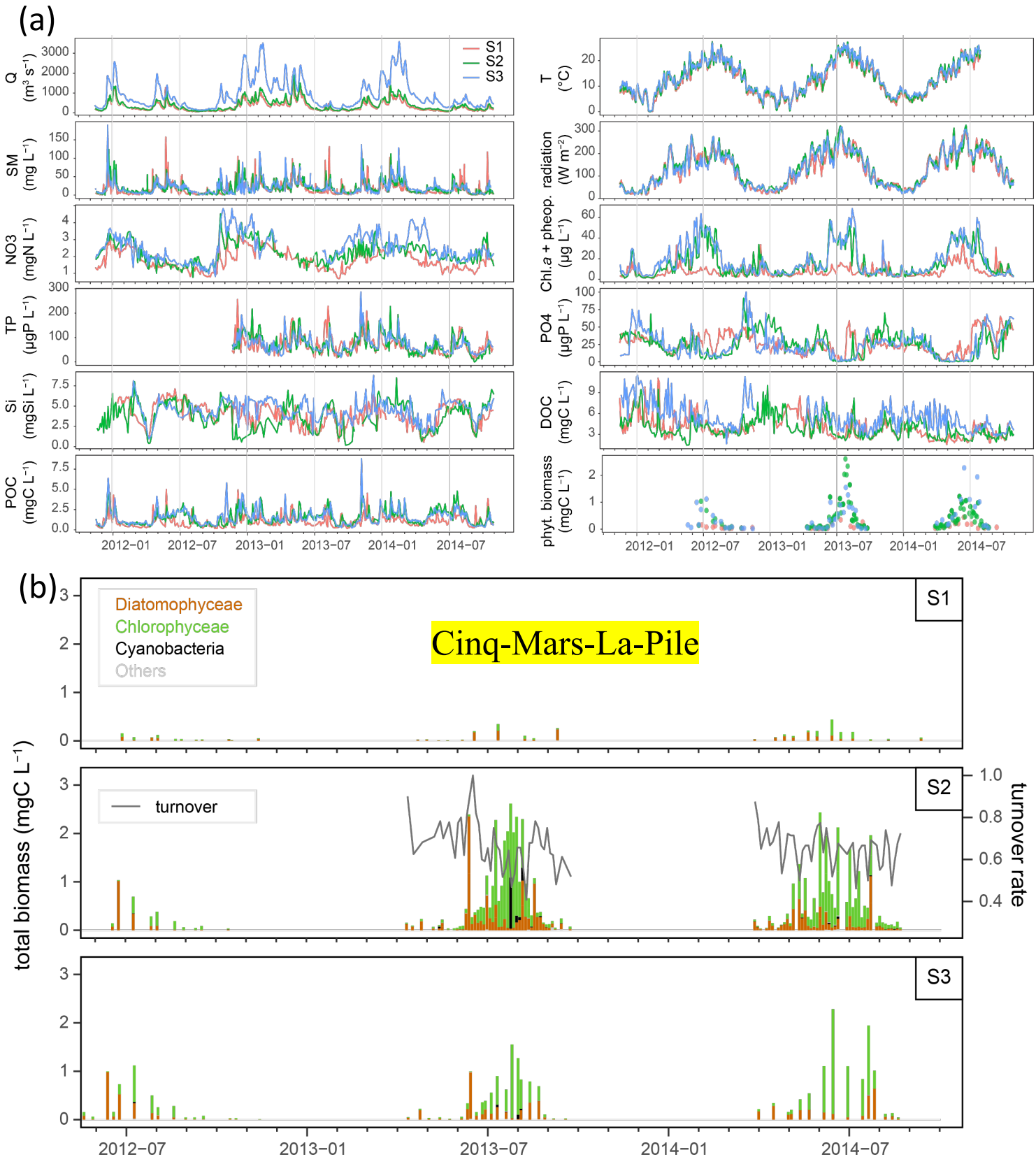
(a)
Q (m³ s⁻¹)
SM (mg L⁻¹)
NO3 (mgN L⁻¹)
TP (µgP L⁻¹)
Si (mgSi L⁻¹)
POC (mgC L⁻¹)
S1
S2
S3
T (°C)
radiation (W m⁻²)
Chl.a + pheop. (µg L⁻¹)
PO4 (µgP L⁻¹)
DOC (mgC L⁻¹)
phyt. biomass (mgC L⁻¹)
2012-01
2012-07
2013-01
2013-07
2014-01
2014-07
(b)
Diatomophyceae
Chlorophyceae
Cyanobacteria
Others
Cinq-Mars-La-Pile
S1
S2
S3
turnover
total biomass (mgC L⁻¹)
turnover rate
2012-07
2013-01
2013-07
2014-01
2014-07

Figure S2.

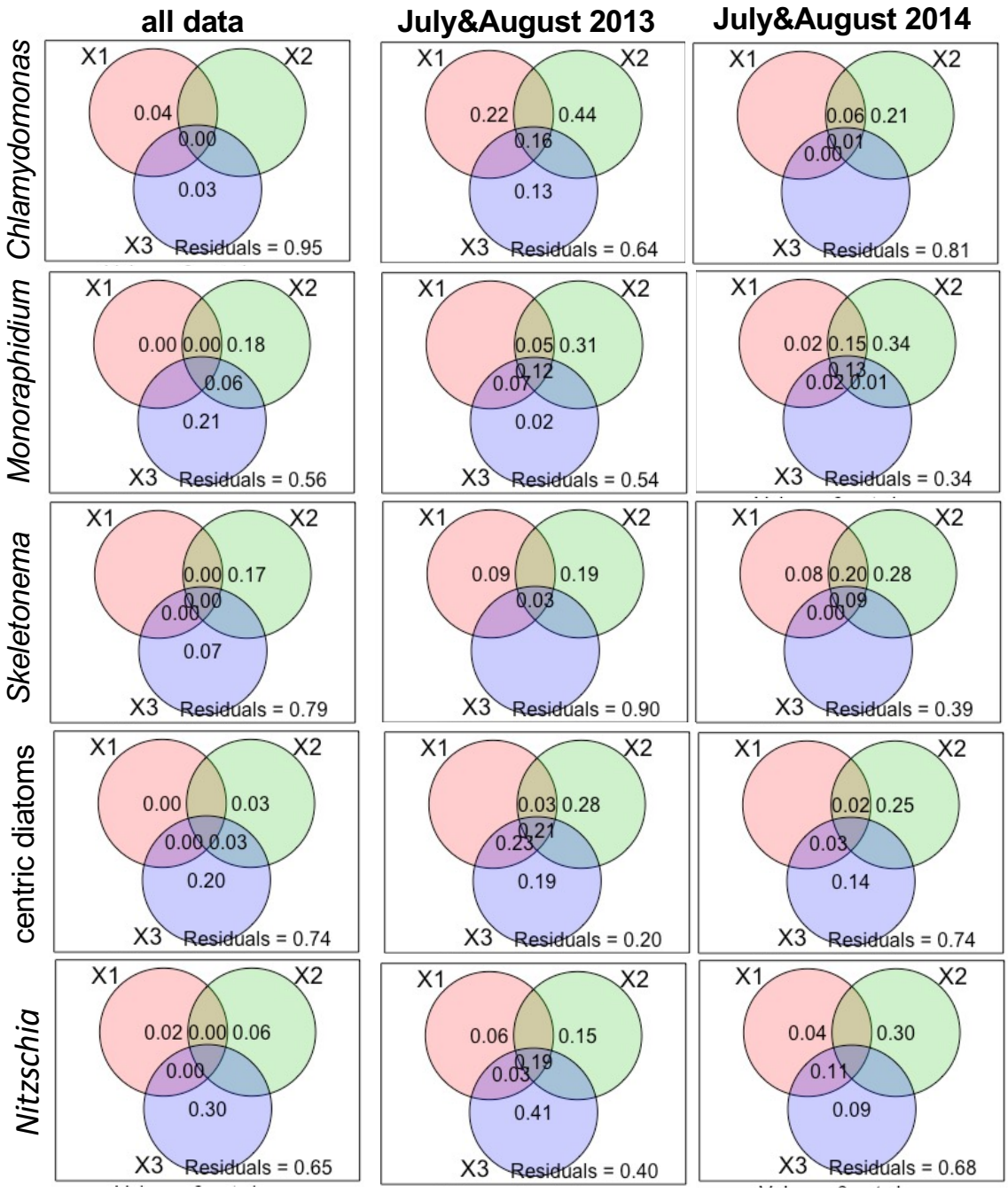
all data
July&August 2013
July&August 2014
Chlamydomonas
Monoraphidium
Skeletonema
centric diatoms
Nitzschia
X1
X2
X3
0.04
0.00
0.03
Residuals = 0.95
0.22
0.44
0.16
0.13
Residuals = 0.64
0.06
0.21
0.01
0.00
Residuals = 0.81
0.00
0.00
0.18
0.06
0.21
Residuals = 0.56
0.05
0.31
0.12
0.07
0.02
Residuals = 0.54
0.02
0.15
0.34
0.13
0.02
0.01
Residuals = 0.34
0.00
0.17
0.00
0.00
0.07
Residuals = 0.79
0.09
0.19
0.03
Residuals = 0.90
0.08
0.20
0.28
0.09
0.00
Residuals = 0.39
0.00
0.03
0.00
0.03
0.20
Residuals = 0.74
0.03
0.28
0.21
0.23
0.19
Residuals = 0.20
0.02
0.25
0.03
0.14
Residuals = 0.74
0.02
0.00
0.06
0.00
0.30
Residuals = 0.65
0.06
0.15
0.19
0.03
0.41
Residuals = 0.40
0.04
0.30
0.11
0.09
Residuals = 0.68